Direct Activation of Toll-like Receptor 4 Signaling in Group 2 Innate Lymphoid Cells Contributes to Inflammatory Responses of Allergic Diseases

Xiao-Dong Li[1], Li She[2], Hamad H. Alanazi[1], Yimin Xu[2], Shuting Guo[3], Qingquan Xiong[3], Hui Jiang[3], Kexin Mo[3], Jingwei Wang[2], Daniel P. Chupp[1], Hong Zan[1], Zhenming Xu[1], Yilun Sun[1], Na Xiong[1], Nu Zhang[1], Zhihai Xie[2], Weihong Jiang[2], Xin Zhang[2], and Yong Liu[2]

[1]The University of Texas Health Science Center at San Antonio Department of Microbiology Immunology and Molecular Genetics
[2]Central South University
[3]Guangzhou Medical University

October 13, 2022

Abstract

Group 2 innate lymphoid cells (ILC2) play a critical role in type 2 immunity. Although their classical activators are known to be host epithelial-derived alarmin cytokines released from tissue damage at barrier sites during microbial infections and allergen exposures, it remains elusive whether ILC2 cells can be directly activated by microbial ligands. Here we examined a number of microbial ligands and identified lipopolysaccharides (LPS) from multiple species of Gram-negative bacteria potently stimulated the cultured human ILC2 to proliferate and produce massive amounts of type 2 effector cytokines IL-5 and IL-13. RNA-seq data revealed a remarkably similar set of type 2 immune responsive genes induced by LPS and IL-33. However, blocking IL-33 receptor signaling failed to decrease the effects of LPS. In contrast, blocking TLR4 receptor, NF-kB and JAK pathways completely abolished the growth and function of LPS-treated human ILC2. Furthermore, ILC2 cells of TLR4 deficient mice were unable to respond to LPS treatment in vitro and in vivo. Importantly, patients with allergic rhinitis, atopic dermatitis and bacteremia had an increased number of peripheral blood ILC2 cells that correlated with elevated serum endotoxin. Collectively, these findings support a non-canonical mode of direct activation of human ILC2 cells via the LPS-TLR4-NF-kB/JAK signaling axis, which is independent of the classical IL-33-ST2 pathway. Thus, targeting TLR4 signaling pathway might be developed as an alternative approach to treat microbial infection-associated and ILC2-mediated inflammatory conditions.

Introduction

Allergic disorders including asthma, allergic rhinitis and atopic dermatitis (AAA) are common diseases affecting more than 300 million people worldwide [1-3]. Although AAA diseases are traditionally characterized by an overzealous Th2-mediated inflammatory response, it has become increasingly appreciated in recent years that group 2 innate lymphoid cells (ILC2) play an important role in the initiation and orchestration of type 2 immunopathologies [4]. ILC2 cells are the innate counterparts of Th2 lymphocytes, but lack rearranged antigen receptors[4-7]. In response to three classical activators, alarmin cytokines IL-33, IL-25 and TSLP, ILC2 cells promptly produce huge amounts of type 2 effector cytokines such as IL-5 and IL-13, which drive the development of type 2 immunopathologies featured by eosinophilia, airway remodeling and mucus hypersecretion [8-11].

Environmental allergens are very complex and often contaminated with microbial or parasitic products

such as lipopolysaccharide (LPS), also known as endotoxin or chitin, so called pathogen-associated molecular patterns (PAMPs). PAMPs could stimulate innate immune cells through binding and activating their corresponding pattern recognition receptors (PRRs). Besides sensing PAMPs, PRRs can also recognize self-ligands, namely damage-associated molecular patterns (DAMPs)[12-15]. Toll-like receptors (TLRs) are the first class of PRRs. All TLRs contain extracellular leucine-rich repeats (LRRs) for ligand bindings and an intracellular Toll-interleukin-1 receptor (TIR) domain that recruits MyD88 and other adaptor proteins to activate signaling cascades, which culminate in the production of various pro- or anti-inflammatory cytokines. To date, 10 TLRs (TLR1–10) have been identified in humans and 12 (TLR1–9, TLR11–13) in mice[16]. TLR2 forms a heterodimer with TLR1, TLR6 or TLR10 to detect microbial lipopeptides and peptidoglycans. TLR4 detects bacterial LPS while TLR5 recognizes bacterial flagellin. The nucleic acid sensing TLRs include TLR3, TLR7/8, TLR9 and TLR13, which detect double-stranded RNA (e.g. poly[I:C]), R848 or single-stranded RNA (ssRNA), unmethylated CpG DNA (e.g. CpG-A), bacterial 23S rRNA and its derivative, a 13-nt sequence, ISR23, respectively [17].

The immune activation of allergen-associated PAMPs is believed to be commonly involved in the initiation of type 2 inflammation[18-23]. Recent studies have also demonstrated that microbial ligands can activate the corresponding innate immune receptors to protect against eosinophilic airway diseases through the inhibition of ILC2 function[24-26]. TLR4 was previously shown to play a role in regulating type 2 immune responses in mouse studies, however, the underlying mechanism remains poorly understood [27-32]. Emerging evidence suggest that ILC2 cells can express various PRRs including TLRs and Nod2[33-36]. Although the role of PRRs in myeloid cells like monocytes and DCs is well established, it remains poorly understood about the molecular details on how PRRs function in ILC2 cells.

In the course of investigating the responsiveness of the cultured human ILC2 cells to various TLR ligands, we determined that LPS robustly triggered human ILC2 to expand and produce type 2 effector cytokinesIL-5 and IL-13. Our RNA-seq data revealed that LPS-induced genes significantly overlapped with those induced by IL-33. However, the blockade of TLR4 signaling, not the canonical IL-33 receptor signaling, completely abolished the activation of ILC2 cells stimulated by LPS. Our findings support a non-classical mode of direct activating human ILC2 cells by the TLR4 signaling without the involvement of IL-33-ST2 pathway.

Results

LPS potently activates the proliferation and cytokine production of human ILC2 cells

ILC2 cells are known to be primarily activated by alarmin cytokines IL-33, TSLP or IL-25. However, it remains elusive whether a single TLR ligand is sufficient to activate human ILC2 cells. To address this issue, various TLR agonists were tested to activate the in vitro-cultured human (CD45+Lin-CRTH2+CD127+) or mouse (CD45+Lin-T1/ST2+) ILC2 cells, which were originally isolated from human blood and mouse samples by FACS sorting (**Figs. S1A and S2A**). The growth and cytokine production of ILC2 cells were analyzed on day 3 or 5 (all experiments if not specifically indicated) with techniques including microscopic examinations, FACS and ELISA, respectively. Among 8 TLR ligands examined, LPS (*E. coli* 0127:B8) was identified to more potently stimulate human ILC2 cells than mouse counterparts to proliferate (**Figs. 1A, S2B and S3A**), and produce type 2 effector cytokines IL-5 and IL-13 (**Figs. 1B, S2C and S3B**). LPS induced little cell death of human blood and mouse bone marrow-derived ILC2 at a wide range of concentration (0.01-10) μg/ml (**Figs. S1B and S3F**). LPS activated human ILC2 cells in a concentration-dependent manner (**Figs. 1C, D & E**) and promoted their growth as measured by the cell proliferation marker Ki-67 and CSFE labelling (**Figs. 1F & G**). We also carefully examined the effects of LPS at different concentrations on mouse ILC2 cells and observed that LPS at 10 or 100 μg/ml did have a weak stimulating effect on mouse bone marrow-, but not lung-derived ILC2 cells **(Figs. S2D, E, & F and S3C, D & E**). Interestingly, Pam3CSK4, a TLR2 agonist was found to be toxic to human, but stimulatory to mouse ILC2 cells (**Figs. 1A & B, S2B & C and S3A & B**). To further determine whether the LPS from other Gram-negative bacteria has the ability to stimulate human ILC2 cells, we performed similar experiments using LPS extracted from *E. coli*055:B5, *P. aeruginosa* and *S. typhimurium* . These three LPS similarly triggered the growth and cytokine production of both human and mouse bone marrow derived ILC2

cells (**Figs. 2A & B and S4**). Additionally, when cultured in the presence of IL-2 and IL-7, LPS strongly enhanced the growth and cytokine production of ILC2 cells derived from 4 healthy donors; in addition, LPS could even significantly increase the effects of IL-33 in 3 donors (**Fig. 2C**), implying a synergistic effect between LPS and IL-33. Taken together, these data suggest that at proper concentrations, LPS can directly activate both human and mouse ILC2 cells to proliferate and induce the secretion of type 2 effector cytokines IL-5 and IL-13.

RNA-seq analysis reveals that LPS-induced genes in human ILC2 cells overlap significantly with those induced by IL-33

To obtain a global view on LPS-activated human ILC2 cells at the transcriptional level, an RNA-seq analysis was performed. To find the best timepoint to collect samples, we examined the kinetics of selected genes (IL-4, IL-5, IL-13 and TNFα) induced by LPS in comparison to an IL-33 control by RT-qPCR. We found that the peak level of these genes appeared at 6 hours in both treatments (**Fig. S5A**). Therefore, we chose the 6h samples to perform an RNA-seq analysis of the differential expression of all genes (**Fig. 3**). In a volcano-plot analysis, 213 genes were up-regulated whereas 52 genes were down-regulated compared with the control, which was also seen in a heatmap analysis (**Figs. 3A & B**). Further cytokine analysis found that numerous type 2 effector cytokines such as IL-4, IL-5, IL13 and CSF2 were induced and highlighted in red (**Fig. 3C**). To further define the functional connections of the DFGs genes, the KEGG (Kyoto Encyclopedia of Genes and Genomes) pathway enrichment and GOBP (Gene Ontology Biological Process) analyses were performed. We discovered that genes from the LPS-treated samples were significantly enriched in the biological processes highly related to immune modulations by cytokines such as TNF and IL-17 (**Figs. 3D & S5B**). By a direct comparison using gene set enrichment analysis (GSEA), IL-33-upregulated gene set was identified to be statistically significant concordance with those induced by LPS (**Fig. 3E**), sharing more than 50% genes (141 genes) (**Fig. 3F**). Taken together, these results reveal that LPS-induced genes overlap significantly with the gene signature induced by IL-33 in human ILC2 cells.

LPS activates human ILC2 cells via TLR4 receptor without the involvement of IL-33-ST2 pathway

Next, we investigated the involvement of TLR4- and ST2-mediated pathways in LPS-triggered signaling in human ILC2 cells. Although it was reported that human ILC2 cells had a detectable level of TLR4 mRNA and were able to respond to a Mix of TLR-ligands[37], it remains to be determined whether LPS alone can activate human ILC2 cells via TLR4 signaling. To address this question, we analyzed the mRNA and protein expression of TLR4 in ILC2 cells. Compared to other TLRs, TLR4 gene was highly expressed in non-treated human ILC2 cells, indicating the importance of TLR4 signaling in this cell type (**Fig. 4A, left**). Also, the cell surface expression of TLR4 protein, but not CD14, was clearly detected by FACS staining (**Fig. 4A, right**). Chemically, LPS contains three parts: lipid A, O-antigen and core oligosaccharide joined by a covalent bond. Lipid A domain is responsible for the toxicity of Gram- bacteria and binding to TLR4. To determine a specific role of TLR4 receptor in LPS-mediated activating human ILC2 cells, we used a chemically synthesized TLR4 agonist a lipid A analog (CRX-527)[38] and an natural antagonist, LPS-RS, to stimulate or block TLR4-specific signaling, respectively. Given that the CRX-527 solvent DMSO is likely toxic at higher concentrations to cells, DMSO alone at different concentrations was included as controls to rule out its potential compounding effects on ILC2 cells. CRX-527 at 0.1 and 1 μg/ml strongly promoted the growth (**Fig. 4B**) and the production of IL-5 and IL-13 (**Fig. 4C**). Due to the toxic effects of DMSO, CRX-527 at higher concentrations 10 or 100 μg/ml completely lost its stimulating effects. Next, we asked whether the LPS activity could be competitively blocked by LPS-RS, a lipopolysaccharide isolated from the photosynthetic bacterium,*Rhodobacter sphaeroides* , which is incapable to trigger TLR4 signaling [39]. Remarkably, LPS-RS at 50 μg/ml or above almost completely inhibited the biological effects of LPS. It is worth to mention that both LPS and LPS-RS were dissolved in water (**Figs. 4D & E**). To demonstrate that TLR4 signaling is essential for LPS to directly activate ILC2 cells, we studied the LPS responsiveness of bone marrow-derived ILC2 cells isolated from WT and $TLR4^{-/-}$ mice. As expected, we found that $TLR4^{-/-}$ ILC2 was completely unresponsive to LPS stimulation (**Fig. S6**). Next, to further provide in vivo evidence

to support that TLR4 signaling is required for LPS to stimulate ILC2, we systemically delivered LPS into Rag1$^{-/-}$, WT and TLR4$^{-/-}$ mice and found that LPS-induced growth, effector function and ST2 expression of ILC2 was strictly dependent on TLR4 signaling (**Fig. S7**). To further address the possible involvement of IL-33-ST2 pathway, we performed a competitive assay by adding to ILC2 culture with increased amounts of the recombinant protein IL1RL1 to sequester extracellular IL-33 in the media. It turned out that whereas IL1RL1 at 1 and 10 μg/ml significantly blocked the effects of IL-33, it failed to affect the activity of LPS on human ILC2 cells (**Figs 5**). These results indicate that LPS activates human ILC2 cells via TLR4 receptor without the involvement of IL-33-ST2 pathway.

NF- κB and JAK-STAT pathways are critical for LPS to activate human ILC2 cells

The engagement of TLRs often triggers the common signaling cascades leading to the activation of a number of transcription pathways[40]. We next determined which pathway is required for LPS to activate human ILC2 cells. To this end, we performed additional RNA-seq analysis and found that the NF-κB and JAK-STAT signaling pathways were strongly associated with the function of LPS-activated human ILC2 cells **(Fig. 6A**). We continued to determine whether the NF-κB or JAK inhibitors could affect the growth and cytokine production of human ILC2 cells treated with LPS. As expected, NF-κB inhibition with Bay 11-7082 at the concentration between 1 to 100 μM completely blocked the LPS-mediated stimulating effects. A pan-Jak inhibitor also blocked all responses to LPS (**Figs. 6B, C & D**). Similarly, these two inhibitors also blocked IL-33-mediated effect on ILC2 cells (**Figs. 6E, F & G**). These data indicate that the NF-κB- and JAK-dependent pathways contribute significantly to LPS-mediated activation of human ILC2 cells.

LPS promotes the proliferation and function of human ILC2 in humanized mice and patients

Since we have shown that LPS is a potent ILC2 activator in vitro, we next moved on to evaluate whether LPS was able to elicit human ILC2 cells-mediated eosinophilia in vivo. To this end, we developed two humanized mouse models, in which NSG or Rag2$^{-/-}\gamma c^{-/-}$ mice were reconstituted with human ILC2s as illustrated in **Fig. 7A** . Similar models have recently been reported with the IL-33 administration[33,41].

Consistent with our in vitro data, the adoptively transferred human ILC2 cells responded to LPS stimulations, which led to the growth and type 2 cytokine production of human ILC2 cells were significantly increased by LPS treatment shown by the cell number and intracellular cytokine staining in these two mouse strains (**Figs. 7B & C**). Due to a high level of protein sequence homology, human IL-5 could function as mouse IL-5 and was previously used to activate mouse eosinophils[42,43]. Moreover, we also observed that increased number of mouse lung eosinophils in both NSG and Rag2$^{-/-}\gamma c^{-/-}$ mice (**Fig. 7D**). To determine whether LPS plays a role in patients with type 2 inflammatory conditions, we compared the percentage of ILC2 and level of LPS in blood samples from healthy individuals to those from patients with allergic rhinitis (A.R.) and atopic dermatitis (A.D.), in which samples from sepsis patients were used as a positive control. The clinical information of these patients was shown in Supplemental**Tables 1, 2 and 3** . Remarkably, all patients with A.R., A.D. and sepsis had an increased ILC2 percentage (**Figs. 8A & B**) and an elevated LPS level (**Fig. 8C**). Blood ILC2 percentage positively correlated with blood LPS level in each A.R., A.D. and sepsis patient (**Fig. 8D**). These data indicate that LPS may play an important role in the regulation of ILC2-mediated inflammatory diseases.

Discussion

In this study, we have discovered a novel function for LPS-TLR4 signaling in ILC2 cells. LPS extracted from multiple species of Gram-negative bacteria can potently stimulate human ILC2 cells, to proliferate and produce massive amounts of type 2 effector cytokines IL-5 and IL-13. This direct effect on ILC2 cells by LPS-TLR4 signaling axis does not require the classical IL-33-ST2 pathway but rather requires the NF-kB and JAK pathways. In lungs of wild type and humanized mice, LPS can promote the proliferation of the adoptively transferred mouse and human ILC2 cells in a TLR4-signaling dependent manner. Further, the increased number of blood ILC2 seems to correlate well with the elevated level of blood LPS in patients including A.R., A.D. and sepsis. Mechanistically, our RNA-seq data strikingly reveals that LPS upregulates a large set of genes overlapped significantly with those induced by IL-33. To our best knowledge, this is the

first report to demonstrate that LPS-TLR4 signaling directly functions in human ILC2 cells to promote their proliferation and production of type 2 effector cytokines independent of the endogenous IL-33-ST2 pathway.

ILC2 cells are known to be activated by tissues-derived alarmin signals when exposed to environmental allergens. In recent years, accumulating evidence has also suggested that diverse receptors expressed on the surface of ILC2 cells can either enhance or repress their activation and proliferation in response to various non-classical signals, hormones, regulatory cytokines, neuropeptides and lipids[44]. Our findings have identified that TLR4 signaling pathway plays an important role in the survival, proliferation, and the production of type 2 cytokines by human ILC2 cells. Although it was previously shown that human ILC2 cells expressed the mRNA of some TLRs (TLR1, TLR4, and TLR6) and could respond to a mixture of three TLR-ligands[37], it has remained unknown about which TLR pathway actually functions in human ILC2 cells.

Previous epidemiological and experimental studies have suggested that endotoxin-TLR4 signaling contributes to the development of type 2 inflammatory reactions[27,45-48]. However, its underlying cellular and molecular mechanisms remain poorly understood. Natural allergens contain not only allergic proteins, but also various PAMPs derived from bacteria, parasites and viruses, which may stimulate innate immune sensors such as TLRs to participate in the regulation of type 2 inflammatory responses[18-23]. In the current study we have demonstrated that bacterial endotoxin could directly engage TLR4 receptor expressed on the surface of ILC2 cells to robustly activate their proliferation and production of type 2 effector cytokines in culture and in vivo in a humanized mouse model. Besides its classical ligand LPS, other endogenous ligands, so called DAMPs, such as HMGB1[49], hyaluronan[50], OxPAPC[51], surfactant protein A [52], S100 proteins[53], HSP72[54,55]etc. have been reported to act as TLR4 agonists. It has been recently reported that the proteinase-cleavage of fibrinogen could elicits allergic responses through TLR4-mediated pathway[56]. It would be interesting to evaluate whether those self TLR4 ligands are able to activate human ILC2 cell in future studies.

ILC2 cells have the ability to communicate with various cell types through the surface expression of multiple receptors, which can bind to ligands present on other immune cells such as DCs, and T or B cells[44,57,58]. We found in our RNA-seq analysis that LPS treatment alone was sufficient to induce the expression of many members of the tumor necrosis factor receptor superfamily (TNFRSF) and their ligands (TNFSF) in ILC2 cells, which are known to provide key co-stimulatory signals to T- or B cells. However, more work will be needed to understand the function and regulatory mechanisms of how these molecules on ILC2 cells act to interact with other immune cell types to regulate type 2 immunity.

In conclusion, our findings support a new mode of activating human ILC2 cells via the LPS-TLR4 signaling axis without the involvement of its classical activating pathway mediated by IL-33 receptor, IL1RL1. As to the wide availability of TLR4 ligands, which can originate from either a foreign origin such as bacterial infections or an endogenous source like DAMPs, thus, inhibiting TLR4 signaling pathway might be developed as a new approach for improving ILC2-mediated type 2 inflammatory conditions.

Material and methods

Mice

Rag1$^{-/-}$,*Pa*γ*2*$^{-/-}$$\gamma_S^{-/-}$(*Rag2*$^{tm1.1Flv}$*Il2rg*$^{tm1.1Flv}$/ J, 014593) and NSG (NOD.Cg-*Prkdc*^{scid}*Il2rg*^{tm1Wjl} /SzJ, 005557) mice were purchased from Jackson Laboratory. All animals were bred and maintained under specific pathogen-free conditions in the animal facility according to the experimental protocols approved by the Institutional Animal Care and Use Committee.

Regents

The medium used was RPMI 1640 (Sigma) containing 10% FBS (HyClone), 1% penicillin-streptomycin (Gibco), 1x GlutaMAX^{TM}-I (Gibco) and 50 μM 2-Mercaptoethanol (Sigma). PamsCSK4, Poly(I:C), Flagellin, R848 and CpG-A were purchased from InvivoGen. ISR23 was obtained from IDT (Integrated DNA Technologies). LPS from*Escherichia coli* 0127:B8, *Escherichia coli* 055:B5,*Pseudomonas aeruginosa* 10 (*P. aeruginosa*),*Salmonella enterica serotype typhimurium* (*S. typhimurium*) were all purchased from Sigma. Recombinant cytokines IL-2, IL-7 and IL-33 (human and mouse) were from PeproTech. TLR4 agonist:

CRX-527 (tlrl-crx-527) and TLR4 antagonist: LPS-RS Ultrapure (tlrl-prslps) were obtained from InvivoGen. Human IL1RL1/ST2 Protein (isoform a, His Tag) (13034-H08H) was purchased from Sino Biological. NF-κB inhibitor Bay 11-7802 and JAK inhibitor 1 were both from EMD Millipore. PMA and Brefeldin A were purchased from Sigma and BioLegend, respectively.

Isolation of ILC2 cells

Human ILC2s were isolated from peripheral blood of healthy donors or umbilical cord blood samples from healthy full-term births in the Department of Obstetrics and Gynecology of UT Health San Antonio. All human samples were used in compliance with UT Health San Antonio Institutional Review Board. Peripheral or Cord Blood Mononuclear Cells (PBMCs or CBMCs) were isolated from diluted umbilical cord blood (1:2) by density gradient centrifugation using density gradient medium, Histopaque® (Sigma Aldrich) and SepMateTM 50 mL tubes (STEMCELL Technologies) [59]. Cells were then washed once with dPBS-FBS buffer (dPBS, 3% fetal bovine serum, 1mM EDTA) and resuspended in dPBS-FBS. Cells were stained with antibodies against CD45 and lineage markers (CD3, CD14, CD16, CD19, CD20 and CD56), and ILC2 markers CRTH2, CD127 (all from BioLegend). Human ILC2s were sorted by the BD FACSAria cell sorter as CD45+Lin-CRTH2+CD127+ cells. The purity of sorted ILC2s was determined to be greater than 95%. Sorted human ILC2s were cultured and expanded in medium supplemented with rh-IL-2 and rh-IL-7 (all at 50 ng/mL) in 96-well round plates for 6 days before further experiments.

Mouse Lung ILC2s were isolated from *Rag1*$^{-/-}$mice treated with rm-IL-33 (250 ng/mouse) for 3 consecutive days plus 2 days of resting before processing lung tissues for sorting ILC2 cells with an BD FACSAria cell sorter. The criteria for identifying ILC2 is lacking classical lineage markers (CD3ε, CD4, CD8α, CD11c, FceRIα, NK1.1, CD19, TER119, CD5, F4/80 and Gr-1), but expressing markers of CD45 and T1/ST2 (all from BioLegend). The purity of sorted ILC2s should be greater than 95%. Sorted ILC2s were cultured and expanded in medium supplemented with mouse IL-2 and IL-7 (all at 10 ng/mL) in 96-well round plates for 6 days before further experiments.

Culture and treatment of human and mouse ILC2 cells

Sorted human ILC2 were cultured in the medium (200 μl) with or without rh-IL-2, rh-IL-7 and rh-IL-33 (all at 50 ng/ml) in 96-well round plates (500 or 1,000 cells/well) in a 37 incubator with 5% CO_2. Cells were treated with Pam3CSK4, Poly(I:C), LPS, Flagellin, R848, CpG-A and ISR23 (different concentration as indicated) for 3 or 5 days. And the human ILC2 cells were treated with TLR4 agonist or antagonist, human IL1RL1/ST2 Protein (isoform a, His Tag) (added 1 hour prior to the treatment with LPS or IL-33), NF-κB or JAK inhibitor as indicated in figure legends for 5 days. After 3 days treatment, the percentage of IL-5$^+$IL13$^+$ cells, the expression of Ki-67 and cell death of ILC2 cells were analyzed by flow cytometry. After 5 days treatment, the number and proliferation of ILC2 cells were analyzed by flow cytometry, and the levels of cytokines (IL-4, IL-5 and IL-13) in the supernatants were measured by ELISA.

Sorted mouse bone marrow or lung ILC2 were cultured and treated with the same TLR ligands in 200 μl media with or without mouse IL-2, IL-7 and IL-33 (all at 10ng/ml) in 96-well round plates (1,000 cells/well) in a 37 incubator with 5% CO_2. The percentage of IL-5$^+$IL13$^+$ cells, expression of Ki-67 on mouse ILC2 cells were analyzed by flow cytometry 3 days later. The number and proliferation of ILC2 cells were analyzed by flow cytometry 5 days later, and the supernatant were collected for further detecting of IL-5 and IL-13 by ELISA.

Flow cytometric analysis

Fc receptors were blocked with 2.4G2 hybridoma supernatant (generated in the lab). For the detection of early-stage apoptotic cells, Annexin V staining was performed according to the protocol (eBioscience). Intranuclear staining of Ki-67 was performed with the True-Nuclear Transcription Factor Buffer Set (BioLegend) according to the manufacturer's instructions. For intracellular cytokine staining, human or mouse ILC2 cells were cultured and treated as indicated for 3 days, then followed by incubating with Brefeldin A for 3 hours. After surface staining, cells were fixed and permeabilized with BioLegend Cytofix/Perm buffer

and further stained intracellularly with anti-human IL-5 and IL-13, or anti-mouse IL-5 and IL-13, respectively. For lung single-cell suspensions, 2 x 10^6 total live nucleated cells were stimulated in 200 µl media with Brefeldin A and PMA (phorbol 12-myristate 13-acetate) (30 ng/mL) at 37 °C for 3 hours. After surface staining, cells were fixed and permeabilized and further stained intracellularly with anti-human IL-5 and IL-13. Dead cells were stained with eFluor506 Fixable Viability Dye before fixation and permeabilization and excluded during analysis. For TLR4 and CD14 expression on human ILC2 cells, cells were stained with the surface markers anti-Human TLR4 and anti-Human CD14. For CD154 expression, human ILC2 cells were cultured and stimulated as indicated for 5 days, and followed by staining with anti-Human CD154.

Protein quantification in cell culture supernatants

Cytokines (IL-5 and IL-13) in supernatant of human and mouse ILC2 cell cultures were analyzed with ELISA kits from Invitrogen. All final reactions were developed with TMB substrate (Thermo scientific) and stopped by sulfuric acid (0.16M), and the OD at 450 nm was measured.

CSFE staining

Human ILC2 cells were stained with 1 µM CSFE (CSFE cell division tracker kit, BioLegend) according to the manufacturer's recommendations. Followed by cultured in the medium with or without rh-IL-2, rh-IL-7, rh-IL-33 (all at 50 ng/ml) or LPS (10 µg/ml) for 3 or 5 days in a 37 incubator with 5% CO_2. The proliferation of ILC2 cells were analyzed by flow cytometry.

Humanized Mice

Purified human ILC2 cells were cultured with rh-IL-2 and rh-IL-7 (all at 50 ng/ml) for 6 days, and then adoptively transferred to NSG mice or$Rag^{-/-}\gamma c^{-/-}$ mice (4 x 10^4 cells/mouse). 4 hours after cell transfer, host mice were challenged with rh-IL-2&7 (all 250 ng/mouse) in absence or presence of LPS (5 µg/mouse) on day 0, 1, 2 as shown in **Fig. 7A** . On day 5, mice were sacrificed, lung was performed and analyzed.

FACS analysis of lung

Mice were sacrificed at indicated times and the lung tissues were digested in 8 ml RPMI-1640 containing Liberase (50 µg/ml) and DNase I (1 µg/ml) for about 45 min at 37 °C. Cell suspensions were filtered through 70 µm cell strainers and washed once with RPMI-1640. Human ILC2 cells and mouse eosinophils in lung were labeled with antibodies as indicated, then mixed with counting beads for further FACS analysis on BD Celesta cell analyzer. Flow cytometry data were analyzed using FlowJo software. The antibodies and reagents for FACS analysis are listed below: SPHERO AccuCount Fluorescent (ACFP-70-5, Spherotech), Anti-Human CD45 APC-Cy7 (HI30, BioLegend), Anti-Human CRTH2 APC (BM16, BioLegend), Anti-Human CD127 PE (A019D5, BioLegend), Anti-Mouse Siglec-F PE (E50-2440, BD Bioscience), Anti-Mouse CD11c PE-Cy7 (N418, TONBO bioscience), Anti-Mouse CD45 PerCP-Cy5.5 (30-F11, BioLegend), Fixable Viability Dye eFluor 506 (Invitrogen).

Real-Time Quantitative PCR

Human ILC2 cells were treated with or without LPS (10 µg/ml) or rh-IL-33 (50 ng/ml) in 200 µl media with or without rh-IL-2&7 (all 50 ng/ml) for 6 or 16 hours. Total RNA was extracted with TRIzol reagent (Life Technologies) according to the manufacturer's instructions. Reverse transcription and real-time PCR (qPCR) reactions were carried out using iScript cDNA synthesis kit and iQ SYBR Green Supermix (Bio-Rad). qPCR was performed on a Bio-Rad CFX384 Touch? Real-Time PCR Detection System using the following human primers (Forward and Reverse, 5'3'): GAPDH (ATGACATCAAGAAGGTGGTG; CATACCAGGAAATGAGCTTG), IL-4 (ACTTTGAACAGCCTCACAGAG; TTGGAGGCAGCAAAGATGTC), IL-5 (AGCTGCCTACGTGTATGCCA; CAGGAACAGGAATCCTCAGA), IL-13 (TGAGGAGCTGGTCAACATCA; CAGGTTGATGCTCCATACCAT), TNFα (CCTGGTATGAGCCCATCTATCTG; TAGTCGGGCCGATTGATCTC).

RNA isolation, RNA-Seq and Bioinformatics

Purified human ILC2 cells ($4x10^4$) were cultured and stimulated with LPS (10 μg/ml) or recombinant human IL-33 protein (rh-IL-33) (50 ng/ml) in the presence with rh-IL-2&7 (all at 50 ng/ml) for 6 hours. Total RNA was extracted with RNeasy Mini Kit (Qiagen) according to the manufacturer's instructions.

After the quality of RNA samples was verified with an Agilent Bioanalyzer 2100 (Agilent), RNA was further processed using an Illumina TruSeq RNA sample prep kit v2 (Illumina). Clusters were generated using TruSeq Single-Read Cluster Gen. Kit v3-cBot-HS on an Illumina cBot Cluster Generation Station. After the quality control procedures, individual RNA-Seq libraries were pooled based on their respective 6 bp index portion of the TruSeq adapters and sequenced at 50 bp/sequence using an Illumina HiSeq 3000 sequencer. Resulting reads were checked by assurance (QA) pipeline and initial genome alignment (Alignment). After sequencing, demultiplexing with CASAVA was employed to generate a Fastq file for each sample. All sequencing reads were aligned with the (GRCh38/hg38) reference genome using HISAT2 default settings, yielding Bam files, duplicated reads were discarded by using Picard, then were processed using HTSeq-count to obtain counts for each gene. RNA expression levels were determined using GENCODE annotation. Differential expression analysis was performed using the Deseq2 package in R post-normalization based on a Benjamini-Hochberg false discovery rate (FDR)-corrected threshold for statistical significance of padj <0.05 or raw p value <0.01. Transcript read counts were transformed to ln(x+1) used to generate heatmaps in Clustvis. Volcano plots depicting log2-FoldChange and raw or adjusted p values were generated in R. Venn diagram were generated by use the VennDiagram package in R.

To investigate biological pathways, DEGs (Differential Expression Genes) were manually curated and compared to multiple public databases, including Gene Ontology (GO) and Kyoto Encyclopedia of Genes and Genomes (KEGG), for enrichment analysis. For gene set enrichment analysis (GSEA), IL-33 upregulated gene set was identified from our RNASeq data comparing the sample rh-IL-33 in the presence of rh-IL-2&7 with the sample only has rh-IL-2&7 stimulation by using the threshold for statistical significance raw p value <0.01 and log2-FoldChange >1. Samples with or without LPS in the presence of rh-IL-2&7 were directly compared to this gene set to identify statistically significant concordance in the expression using the gene set enrichment analysis (GSEA) algorithm.

ELISA for detecting serum LPS

Peripheral blood samples were collected from healthy donors and patients with allergic rhinitis, atopic dermatitis, and sepsis. The level of serum LPS was analyzed by a highly sensitive ELISA kit according to the manufacture instruction (Cloud-Clone Corp.). Briefly, reagents A and B were sequentially applied. For detection, TMB substrate was finally added. The reaction was stopped by the stop solution provided by the kit. The OD value of each sample was read at 450nm.

Human PBMC **collection and analysis**

Blood sample collections from patients with allergic rhinitis, atopic dermatitis, sepsis, and healthy donors were conducted in compliance with the guideline of Institutional Review Board of Xiangya Hospital at Central South University. A peripheral blood mononuclear cell (PBMC) was isolated from blood samples using Ficoll-Paque PLUS in a 15mL centrifuge tube. The cell faction containing PBMC was pelleted by centrifugation, washed, and suspended with 2% FACS buffer (PBS with 2% FBS). The obtained PBMC was counted with a BIO-RAD cell counting slide in a TC20 Automated Cell Counter. 2x10ˆ6 cells were then transferred into a well of a 96-well round bottom plate. For FACS analysis, cells were stained with Ghost Dye^{TM} Violet 510, FITC anti-human Lineage Cocktail (CD3, CD14, CD16, CD19, CD20, CD56), APC anti-human CD294 (CRTH2), APC/Cyanine7 anti-human CD45, and PE anti-human CD127 (IL-7Rα) and analyzed by flow cytometry.

Statistical analysis

The statistical analysis was done using software GraphPad Prism 6. For comparison of two groups, P values were determined by unpaired two-tailed Student's t test. For comparison of more than two groups, Two-Way ANOVA was performed. P values are indicated on plots and in figure legends. P value<0.05 was considered

statistically significant. (P value [?]0.05 was not considered statistically significant [N.S.]. * $p < 0.05$, ** $p < 0.01$, *** $p < 0.001$, **** $p < 0.0001$).

Acknowledgements

We thank Ms. Karla Gorena, Mr. Sebastian Montagnino for technical assistance in flow cytometry and FACS sorting. We thank Drs. Zhao Lai, Yi Zou, and Yidong Chen for RNA-seq analysis and informatics assistance. L.S. is supported by the China Scholarship Council and Hunan Provincial Innovation Foundation for Postgraduate (CX2017B068). L.S., X.Z., Y.L. and X.-D.L. are supported by National Natural Science Foundation of China (Nos. 82073009, 81974424, 81874133, 81773243, 81772903, 81602389, and 82270022). H.H.A. is supported by the Department of Clinical Laboratory Sciences, College of Applied Medical Sciences, Jouf University, Sakaka, Saudi Arabia. X.-D.L. is supported by the Max and Minnei Voelcker Fund and Guangzhou Medical University Startup Fund.

Author contributions

L.S., H.H.A. and Y. X. performed most experiments; L.S., H.H.A., Y.X., J.W., D.P.C., Y.X., H.Z., Z.X., Y.S., N.X., W.J., Z.X., X.Z., Y.L. and X.-D.L. analyzed data; L.S., H.H.A., Y.L. and X.-D.L. planned, designed research. L.S., Y.L. and X.-D.L. wrote the manuscript; All authors discussed the results and participated in writing and commenting on the manuscript.

Competing interests: The authors declare no conflict of interest.

References

1. Jackson KD, Howie LD, Akinbami LJ. Trends in allergic conditions among children: United States, 1997-2011.*NCHS Data Brief.* 2013(121):1-8.

2. Kay AB. Allergy and allergic diseases. First of two parts. *N Engl J Med.* 2001;344(1):30-37.

3. Kay AB. Allergy and allergic diseases. Second of two parts. *N Engl J Med.* 2001;344(2):109-113.

4. Vivier E, Artis D, Colonna M, et al. Innate Lymphoid Cells: 10 Years On. *Cell.*2018;174(5):1054-1066.

5. Eberl G, Colonna M, Di Santo JP, McKenzie AN. Innate lymphoid cells. Innate lymphoid cells: a new paradigm in immunology. *Science.* 2015;348(6237):aaa6566.

6. Artis D, Spits H. The biology of innate lymphoid cells. *Nature.* 2015;517(7534):293-301.

7. Barlow JL, McKenzie ANJ. Innate Lymphoid Cells of the Lung. *Annu Rev Physiol.* 2019;81:429-452.

8. Liew FY, Girard JP, Turnquist HR. Interleukin-33 in health and disease. *Nat Rev Immunol.*2016;16(11):676-689.

9. Cayrol C, Girard JP. Interleukin-33 (IL-33): A nuclear cytokine from the IL-1 family. *Immunol Rev.*2018;281(1):154-168.

10. Kubo M. Innate and adaptive type 2 immunity in lung allergic inflammation. *Immunol Rev.*2017;278(1):162-172.

11. Molofsky AB, Savage AK, Locksley RM. Interleukin-33 in Tissue Homeostasis, Injury, and Inflammation.*Immunity.* 2015;42(6):1005-1019.

12. Akira S, Uematsu S, Takeuchi O. Pathogen recognition and innate immunity. *Cell.*2006;124(4):783-801.

13. Wu J, Chen ZJ. Innate immune sensing and signaling of cytosolic nucleic acids. *Annu Rev Immunol.* 2014;32:461-488.

14. Brubaker SW, Bonham KS, Zanoni I, Kagan JC. Innate immune pattern recognition: a cell biological perspective. *Annu Rev Immunol.* 2015;33:257-290.

15. Man SM, Karki R, Kanneganti TD. AIM2 inflammasome in infection, cancer, and autoimmunity: Role in DNA sensing, inflammation, and innate immunity. *Eur J Immunol.*2016;46(2):269-280.

16. Roach JC, Glusman G, Rowen L, et al. The evolution of vertebrate Toll-like receptors. *Proc Natl Acad Sci U S A.* 2005;102(27):9577-9582.

17. Li XD, Chen ZJ. Sequence specific detection of bacterial 23S ribosomal RNA by TLR13. *Elife.*2012;1:e00102.

18. Locksley RM. Asthma and allergic inflammation. *Cell.* 2010;140(6):777-783.

19. Palm NW, Rosenstein RK, Medzhitov R. Allergic host defences. *Nature.* 2012;484(7395):465-472.

20. Stewart GA, Thompson PJ. The biochemistry of common aeroallergens. *Clin Exp Allergy.*1996;26(9):1020-1044.

21. Van Dyken SJ, Mohapatra A, Nussbaum JC, et al. Chitin activates parallel immune modules that direct distinct inflammatory responses via innate lymphoid type 2 and gammadelta T cells. *Immunity.* 2014;40(3):414-424.

22. Van Dyken SJ, Liang HE, Naikawadi RP, et al. Spontaneous Chitin Accumulation in Airways and Age-Related Fibrotic Lung Disease. *Cell.* 2017;169(3):497-509 e413.

23. Van Dyken SJ, Garcia D, Porter P, et al. Fungal chitin from asthma-associated home environments induces eosinophilic lung infiltration. *J Immunol.* 2011;187(5):2261-2267.

24. Thio CL, Lai AC, Chi PY, Webster G, Chang YJ. Toll-like receptor 9-dependent interferon production prevents group 2 innate lymphoid cell-driven airway hyperreactivity.*J Allergy Clin Immunol.* 2019.

25. Maazi H, Banie H, Aleman Muench GR, et al. Activated plasmacytoid dendritic cells regulate type 2 innate lymphoid cell-mediated airway hyperreactivity. *J Allergy Clin Immunol.* 2018;141(3):893-905 e896.

26. Sabatel C, Radermecker C, Fievez L, et al. Exposure to Bacterial CpG DNA Protects from Airway Allergic Inflammation by Expanding Regulatory Lung Interstitial Macrophages.*Immunity.* 2017;46(3):457-473.

27. Trompette A, Divanovic S, Visintin A, et al. Allergenicity resulting from functional mimicry of a Toll-like receptor complex protein. *Nature.*2009;457(7229):585-588.

28. McAlees JW, Whitehead GS, Harley IT, et al. Distinct Tlr4-expressing cell compartments control neutrophilic and eosinophilic airway inflammation. *Mucosal Immunol.* 2015;8(4):863-873.

29. Eisenbarth SC, Piggott DA, Huleatt JW, Visintin I, Herrick CA, Bottomly K. Lipopolysaccharide-enhanced, toll-like receptor 4-dependent T helper cell type 2 responses to inhaled antigen. *J Exp Med.*2002;196(12):1645-1651.

30. Deckers J, De Bosscher K, Lambrecht BN, Hammad H. Interplay between barrier epithelial cells and dendritic cells in allergic sensitization through the lung and the skin.*Immunol Rev.* 2017;278(1):131-144.

31. Hammad H, Lambrecht BN. Barrier Epithelial Cells and the Control of Type 2 Immunity. *Immunity.*2015;43(1):29-40.

32. Hammad H, Chieppa M, Perros F, Willart MA, Germain RN, Lambrecht BN. House dust mite allergen induces asthma via Toll-like receptor 4 triggering of airway structural cells.*Nat Med.* 2009;15(4):410-416.

33. Crellin NK, Trifari S, Kaplan CD, Satoh-Takayama N, Di Santo JP, Spits H. Regulation of cytokine secretion in human CD127(+) LTi-like innate lymphoid cells by Toll-like receptor 2. *Immunity.* 2010;33(5):752-764.

34. Hardman CS, Chen YL, Salimi M, et al. IL-6 effector function of group 2 innate lymphoid cells (ILC2) is NOD2 dependent. *Sci Immunol.* 2021;6(59).

35. Hardman CS, Chen YL, Salimi M, et al. CD1a presentation of endogenous antigens by group 2 innate lymphoid cells. *Sci Immunol.* 2017;2(18).

36. Ishii T, Muroi M, Horiguchi K, Tanamoto KI, Nagase T, Yamashita N. Activation through toll-like receptor 2 on group 2 innate lymphoid cells can induce asthmatic characteristics. *Clin Exp Allergy.* 2019;49(12):1624-1632.

37. Maggi L, Montaini G, Mazzoni A, et al. Human circulating group 2 innate lymphoid cells can express CD154 and promote IgE production. *J Allergy Clin Immunol.*2017;139(3):964-976 e964.

38. Stover AG, Da Silva Correia J, Evans JT, et al. Structure-activity relationship of synthetic toll-like receptor 4 agonists. *J Biol Chem.* 2004;279(6):4440-4449.

39. Coats SR, Pham TT, Bainbridge BW, Reife RA, Darveau RP. MD-2 mediates the ability of tetra-acylated and penta-acylated lipopolysaccharides to antagonize Escherichia coli lipopolysaccharide at the TLR4 signaling complex. *J Immunol.*2005;175(7):4490-4498.

40. Kaisho T, Akira S. Toll-like receptor function and signaling. *J Allergy Clin Immunol.*2006;117(5):979-987; quiz 988.

41. Hurrell BP, Galle-Treger L, Jahani PS, et al. TNFR2 Signaling Enhances ILC2 Survival, Function, and Induction of Airway Hyperreactivity. *Cell Rep.*2019;29(13):4509-4524 e4505.

42. Ingley E, Cutler RL, Fung MC, Sanderson CJ, Young IG. Production and purification of recombinant human interleukin-5 from yeast and baculovirus expression systems. *Eur J Biochem.* 1991;196(3):623-629.

43. Tavernier J, Cornelis S, Devos R, Guisez Y, Plaetinck G, Van der Heyden J. Structure/function analysis of human interleukin 5 and its receptor. *Agents Actions Suppl.*1995;46:23-34.

44. Hurrell BP, Shafiei Jahani P, Akbari O. Social Networking of Group Two Innate Lymphoid Cells in Allergy and Asthma. *Front Immunol.* 2018;9:2694.

45. Janeway CA, Jr. Approaching the asymptote? Evolution and revolution in immunology. *Cold Spring Harb Symp Quant Biol.* 1989;54 Pt 1:1-13.

46. Idzko M, Hammad H, van Nimwegen M, et al. Extracellular ATP triggers and maintains asthmatic airway inflammation by activating dendritic cells. *Nat Med.*2007;13(8):913-919.

47. Kool M, Willart MA, van Nimwegen M, et al. An unexpected role for uric acid as an inducer of T helper 2 cell immunity to inhaled antigens and inflammatory mediator of allergic asthma. *Immunity.* 2011;34(4):527-540.

48. Schuijs MJ, Willart MA, Vergote K, et al. Farm dust and endotoxin protect against allergy through A20 induction in lung epithelial cells. *Science.*2015;349(6252):1106-1110.

49. Tang AH, Brunn GJ, Cascalho M, Platt JL. Pivotal advance: endogenous pathway to SIRS, sepsis, and related conditions. *J Leukoc Biol.* 2007;82(2):282-285.

50. Jiang D, Liang J, Fan J, et al. Regulation of lung injury and repair by Toll-like receptors and hyaluronan. *Nat Med.* 2005;11(11):1173-1179.

51. Imai Y, Kuba K, Neely GG, et al. Identification of oxidative stress and Toll-like receptor 4 signaling as a key pathway of acute lung injury. *Cell.* 2008;133(2):235-249.

52. Guillot L, Balloy V, McCormack FX, Golenbock DT, Chignard M, Si-Tahar M. Cutting edge: the immunostimulatory activity of the lung surfactant protein-A involves Toll-like receptor 4. *J Immunol.* 2002;168(12):5989-5992.

53. Vogl T, Propper C, Hartmann M, et al. S100A12 is expressed exclusively by granulocytes and acts independently from MRP8 and MRP14. *J Biol Chem.*1999;274(36):25291-25296.

54. Chase MA, Wheeler DS, Lierl KM, Hughes VS, Wong HR, Page K. Hsp72 induces inflammation and regulates cytokine production in airway epithelium through a TLR4- and NF-kappaB-dependent mechanism. *J Immunol.* 2007;179(9):6318-6324.

55. Wheeler DS, Chase MA, Senft AP, Poynter SE, Wong HR, Page K. Extracellular Hsp72, an endogenous DAMP, is released by virally infected airway epithelial cells and activates neutrophils via Toll-like receptor (TLR)-4. *Respir Res.*2009;10:31.

56. Millien VO, Lu W, Shaw J, et al. Cleavage of fibrinogen by proteinases elicits allergic responses through Toll-like receptor 4. *Science.* 2013;341(6147):792-796.

57. Klose CSN, Artis D. Innate lymphoid cells control signaling circuits to regulate tissue-specific immunity. *Cell Res.* 2020;30(6):475-491.

58. Gurram RK, Zhu J. Orchestration between ILC2s and Th2 cells in shaping type 2 immune responses. *Cell Mol Immunol.* 2019;16(3):225-235.

59. Grievink HW, Luisman T, Kluft C, Moerland M, Malone KE. Comparison of Three Isolation Techniques for Human Peripheral Blood Mononuclear Cells: Cell Recovery and Viability, Population Composition, and Cell Functionality. *Biopreserv Biobank.* 2016;14(5):410-415.

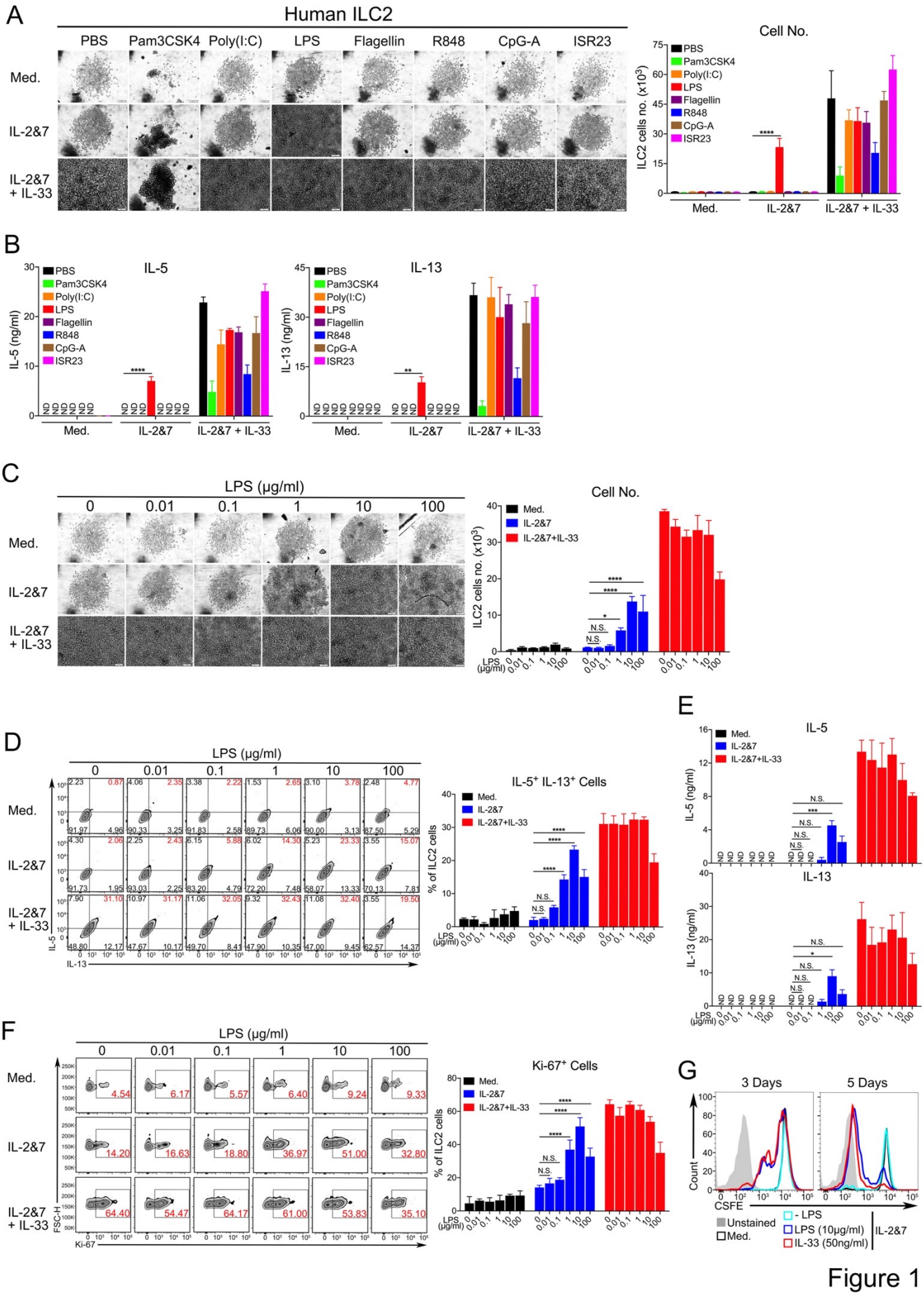
A
Human ILC2
PBS
Pam3CSK4
Poly(I:C)
LPS
Flagellin
R848
CpG-A
ISR23
Med.
IL-2&7
IL-2&7 + IL-33
Cell No.
ILC2 cells no. (x10³)
Med.
IL-2&7
IL-2&7 + IL-33
B
IL-5
IL-13
IL-5 (ng/ml)
IL-13 (ng/ml)
C
LPS (μg/ml)
0
0.01
0.1
1
10
100
Med.
IL-2&7
IL-2&7+IL-33
D
IL-5⁺ IL-13⁺ Cells
% of ILC2 cells
E
IL-5
IL-13
F
Ki-67⁺ Cells
Ki-67
FSC-H
G
3 Days
5 Days
Count
CSFE
Unstained
Med.
- LPS
LPS (10μg/ml)
IL-33 (50ng/ml)
IL-2&7

Figure 1

Figure 1. LPS strongly stimulated the growth and cytokine production of human ILC2. A. Light microscopic images showing the growth of ILC2 cells. FACS sorted human ILC2 cells were treated with various TLR ligands as indicated in a 96-well round-bottom plate for 5 days. Each image represented one well in which 1,000 cells were initially seeded. Scale bar, 100 μm (Left). The number of human ILC2 cells from each treatment was quantified by FACS analysis (Right). **B**. ELISA measuring the production of IL-5 and IL-13 by human ILC2 cells treated with various TLR ligands as indicated. **C.** LPS stimulated human ILC2 cells in a dose-dependent manner. Light microscopic images showing the growth of ILC2 cells treated with the increased dose of LPS as indicated (Left). The number of human ILC2 cells from each dose of LPS treatment was quantified by FACS analysis (Right). **D**. The representative FACS result showing the intracellular staining of IL5+IL13+-double positive human ILC2 cells activated by the increased dose of LPS (Left). The percentage of human ILC2 cells from each dose of LPS treatment was quantified by FACS analysis (Right). **E.** ELISA measuring the production of IL-5 and IL-13 by human ILC2 cells treated with the increased dose of LPS. **F.** The proliferation of LPS-treated human ILC2 cells were analyzed with Ki-67 staining. The representative FACS gating images and quantification of Ki-67 positive cells were shown. The result is a representative of three independent experiments. **G.** CSFE labelling for tacking the proliferation of human ILC2 cells treated with LPS or IL-33 for 3 or 5 days. (P value≥0.05 was considered statistically insignificant, N.S., two-way ANOVA, ** $p < 0.05$, ** $p < 0.01$, *** $p < 0.001$, **** $p < 0.0001$).

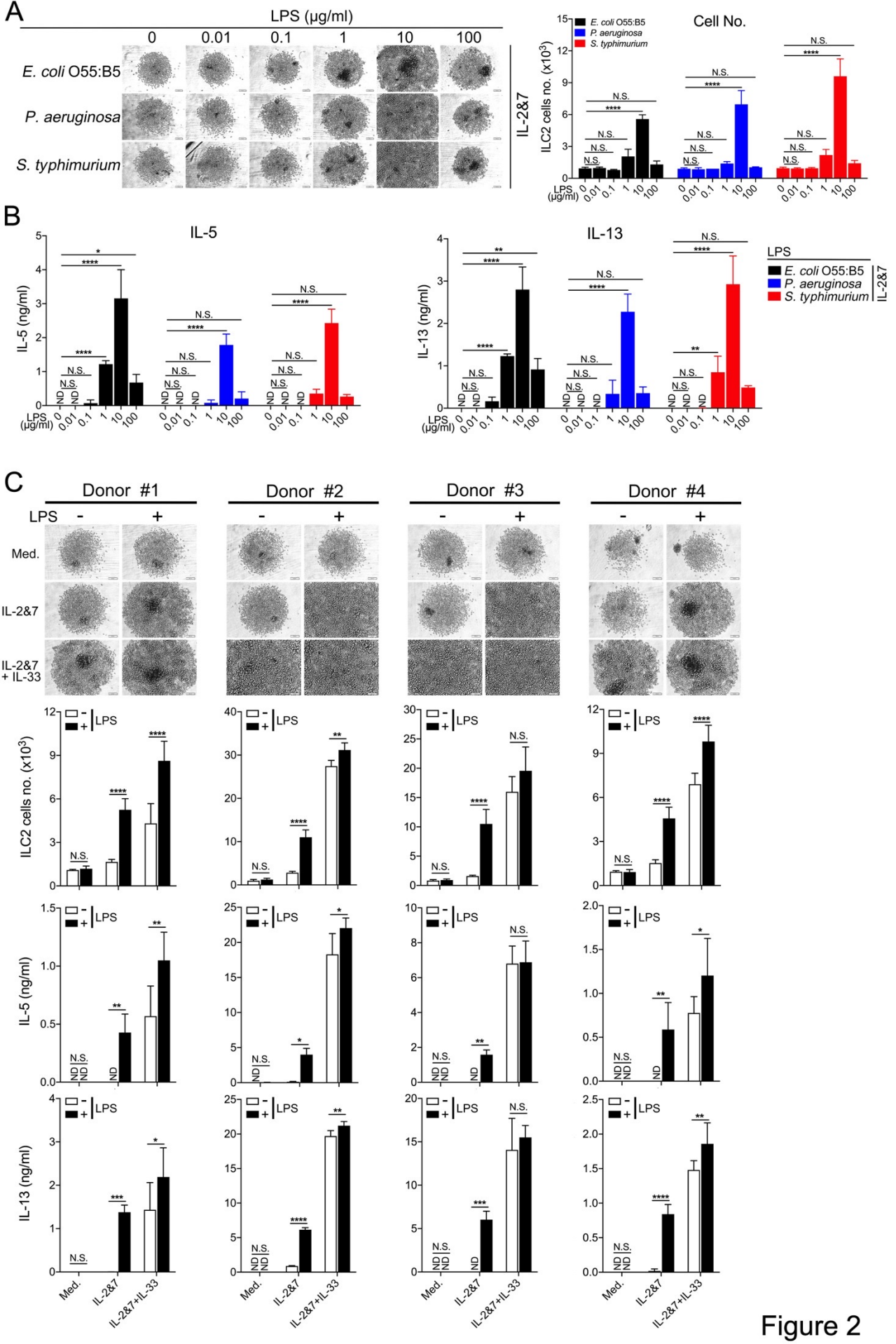
A
LPS (μg/ml)
0
0.01
0.1
1
10
100
E. coli O55:B5
P. aeruginosa
S. typhimurium
IL-2&7
Cell No.
ILC2 cells no. (x10³)
B
IL-5
IL-5 (ng/ml)
IL-13
IL-13 (ng/ml)
LPS
E. coli O55:B5
P. aeruginosa
S. typhimurium
IL-2&7
C
Donor #1
Donor #2
Donor #3
Donor #4
LPS
Med.
IL-2&7
IL-2&7 + IL-33
ILC2 cells no. (x10³)
IL-5 (ng/ml)
IL-13 (ng/ml)
N.S.
ND
Med.
IL-2&7
IL-2&7+IL-33

Figure 2

Figure 2. LPS from various Gram (-) bacterial species could stimulate the growth and cytokine production of human ILC2 from different individuals. A. Light microscopic images showing the growth of ILC2 cells treated with LPS isolated from *E. coli 055:B5*, *P. aeruginosa* and *S. typhimurium*. FACS sorted human ILC2 cells were treated with various LPS as indicated in a 96-well round-bottom plate for 5 days. Each image represented one well in which 1,000 cells were initially seeded. Scale bar, 100 μm (Right). The number of human ILC2 cells treated with various LPS as indicated was quantified by FACS analysis (Right). **B**. ELISA measuring the production of IL-5 and IL-13 by human ILC2 cells treated with various LPS as indicated. **C.** LPS responsiveness of human ILC2 cells from four healthy donors was measured by the growth and production of type 2 effector cytokines. Light microscopic images showing the growth of ILC2 cells derived from 4 individual donors were activated by LPS or IL-33. Each image represented one well in which 1,000 cells were initially seeded. Scale bar, 100 μm (Top). The number of human ILC2 cells derived from 4 individual donors as indicated was quantified by FACS analysis (Middle). ELISA measuring the production of IL-5 and IL-13 by human ILC2 cells derived from 4 individual donors (bottom). (P value≥0.05 was considered statistically insignificant, N.S., two-way ANOVA, * $p < 0.05$, ** $p < 0.01$, *** $p < 0.001$, **** $p < 0.0001$).

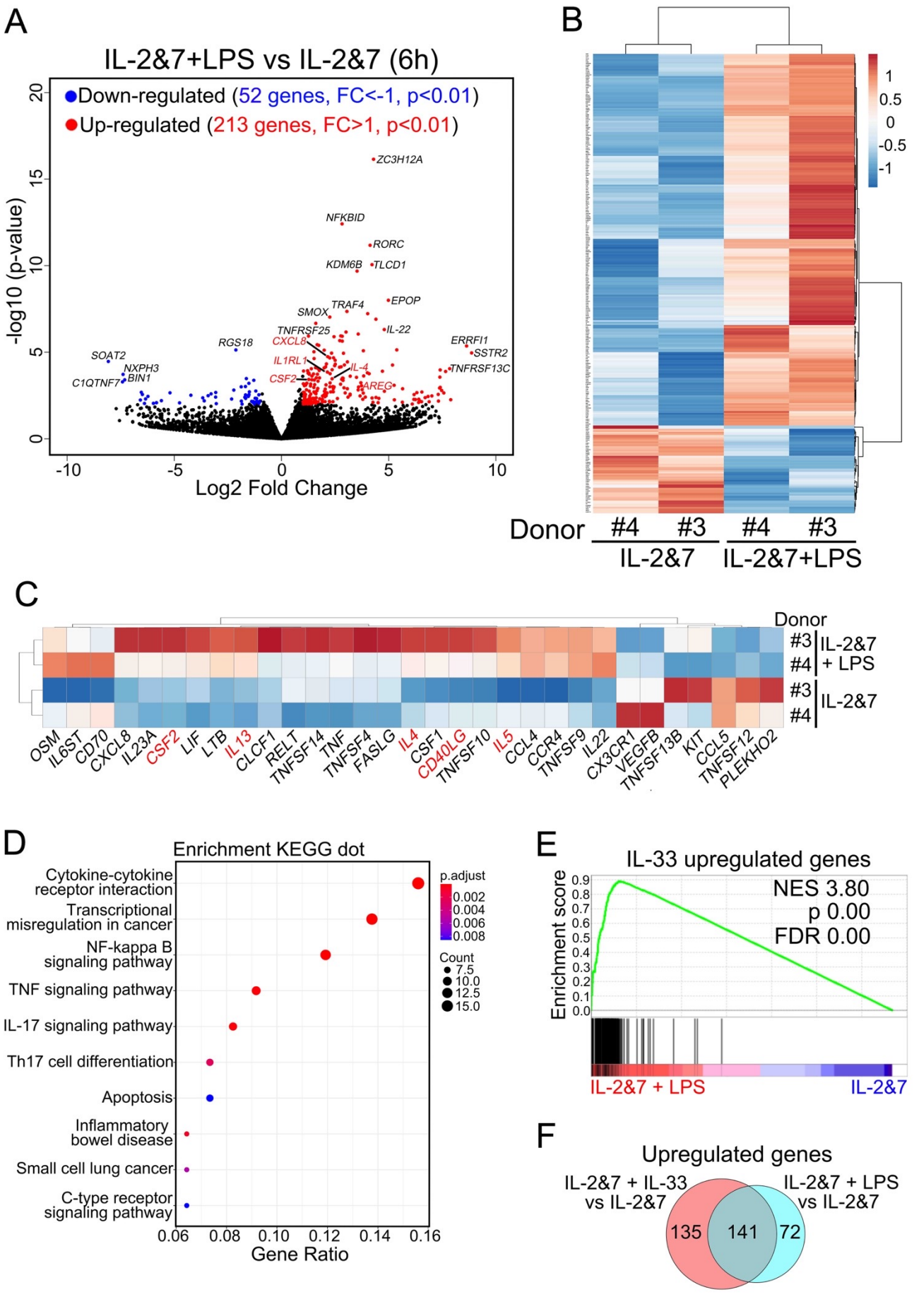
A
IL-2&7+LPS vs IL-2&7 (6h)
Down-regulated (52 genes, FC<-1, p<0.01)
Up-regulated (213 genes, FC>1, p<0.01)
-log10 (p-value)
Log2 Fold Change
ZC3H12A
NFKBID
RORC
KDM6B
TLCD1
EPOP
TRAF4
SMOX
IL-22
TNFRSF25
CXCL8
RGS18
ERRFI1
SSTR2
SOAT2
NXPH3
BIN1
C1QTNF7
IL1RL1
IL-4
CSF2
AREG
TNFRSF13C
B
Donor
#4
#3
#4
#3
IL-2&7
IL-2&7+LPS
C
Donor
#3
#4
IL-2&7 + LPS
#3
#4
IL-2&7
OSM
IL6ST
CD70
CXCL8
IL23A
CSF2
LIF
LTB
IL13
CLCF1
RELT
TNFSF14
TNF
TNFSF4
FASLG
IL4
CSF1
CD40LG
TNFSF10
IL5
CCL4
CCR4
TNFSF9
IL22
CX3CR1
VEGFB
TNFSF13B
KIT
CCL5
TNFSF12
PLEKHO2
D
Enrichment KEGG dot
Cytokine-cytokine receptor interaction
Transcriptional misregulation in cancer
NF-kappa B signaling pathway
TNF signaling pathway
IL-17 signaling pathway
Th17 cell differentiation
Apoptosis
Inflammatory bowel disease
Small cell lung cancer
C-type receptor signaling pathway
Gene Ratio
p.adjust
Count
E
IL-33 upregulated genes
Enrichment score
NES 3.80
p 0.00
FDR 0.00
IL-2&7 + LPS
IL-2&7
F
Upregulated genes
IL-2&7 + IL-33 vs IL-2&7
IL-2&7 + LPS vs IL-2&7
135
141
72

Figure 3

Figure 3. RNA-seq analysis reveals that LPS upregulated genes significantly overlapped with those upregulated by IL-33 in human ILC2 cells . A. Volcano plot showing the up- and down-regulated genes in human ILC2 cells 6 hours after LPS treatment. **B.** Heatmap showing the differentially expressed genes (DEGs) in LPS-activated human ILC2 cells. **C.** Heatmap showing the selected cytokines genes in LPS-activated human ILC2 cells, in which genes related to type 2 immunity are highlighted in red. **D.** Dotplot showing the enrichment analysis of Kyoto Encyclopedia of Genes and Genomes (KEGG). **E.** GSEA analysis of DEGs upregulated by LPS and IL-33 in human ILC2 cells. **F.** Venn diagram depicting the overlapping and non-overlapping genes upregulated in human ILC2 cells stimulated with either IL-2&7 plus LPS or IL-2&7 plus IL-33, as compared to those treated with IL-2&7.

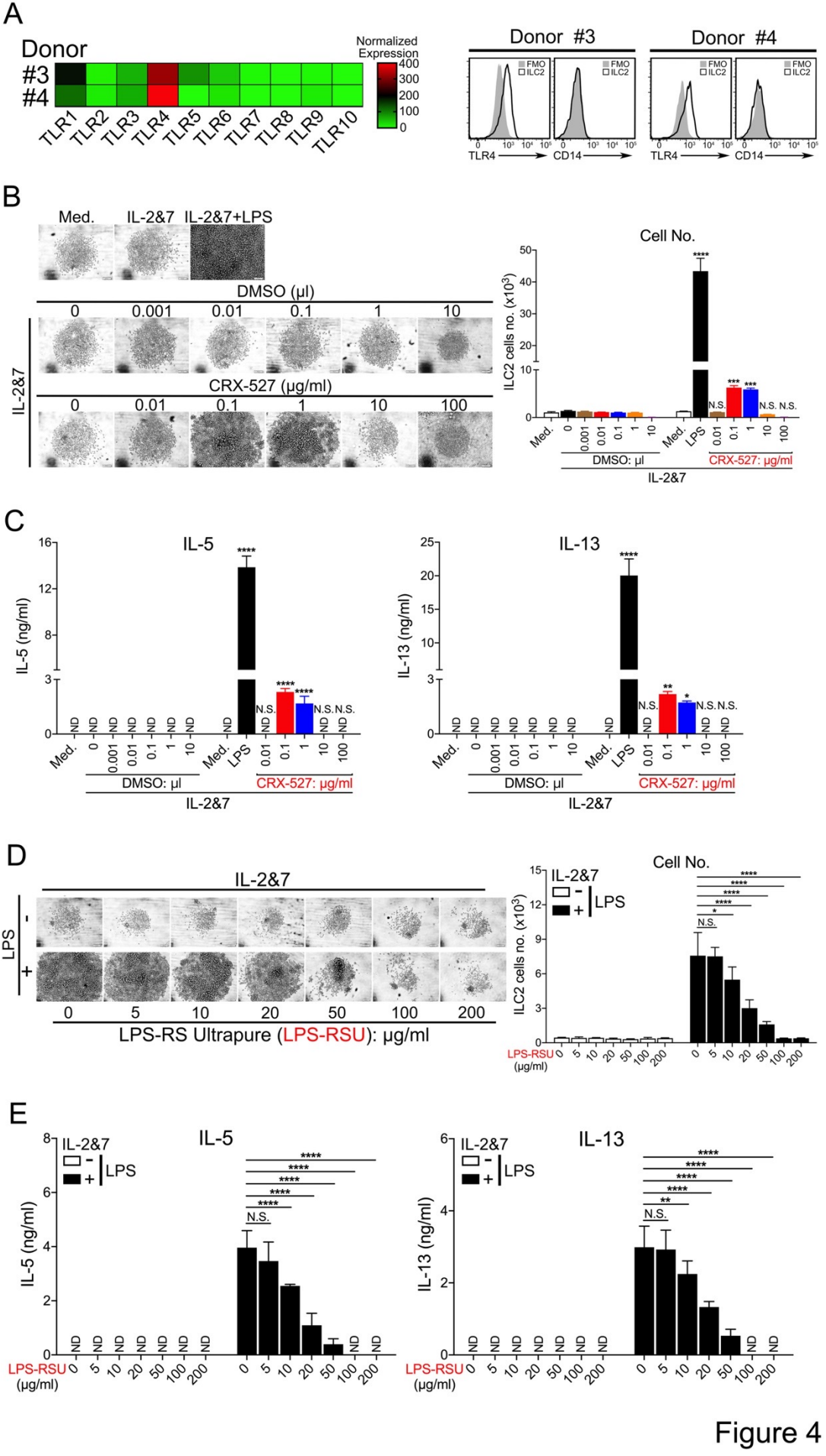
A
Donor
#3
#4
TLR1 TLR2 TLR3 TLR4 TLR5 TLR6 TLR7 TLR8 TLR9 TLR10
Normalized Expression
400
300
200
100
0
Donor #3
Donor #4
FMO
ILC2
TLR4
CD14
B
Med.
IL-2&7
IL-2&7+LPS
DMSO (μl)
0 0.001 0.01 0.1 1 10
IL-2&7
CRX-527 (μg/ml)
0 0.01 0.1 1 10 100
Cell No.
ILC2 cells no. (x10³)
N.S.
DMSO: μl
CRX-527: μg/ml
IL-2&7
C
IL-5
IL-13
IL-5 (ng/ml)
IL-13 (ng/ml)
ND
N.S.
D
IL-2&7
LPS
LPS-RS Ultrapure (LPS-RSU): μg/ml
Cell No.
ILC2 cells no. (x10³)
LPS-RSU (μg/ml)
E
IL-5
IL-13
IL-5 (ng/ml)
IL-13 (ng/ml)
LPS-RSU (μg/ml)

Figure 4

Figure 4. Stimulation and suppression of human ILC2 cells by the synthetic agonist or antagonist of LPS. A. Heatmap showing the normalized mRNA expression level of all 10 human TLRs in human ILC2 cells from two donors (Left). FACS staining of TLR4 or CD14 proteins on the surface of human ILC2 cells (Right). **B.** Light microscopic images showing the growth of ILC2 cells treated with CRX-527, lipid A analog or its solvent DMSO. FACS sorted human ILC2 cells were treated with the increased dose of CRX-527 as indicated. Each image represented one well in which 1,000 cells were initially seeded. Scale bar, 100 μm (Left). The number of human ILC2 cells treated with either CRX-527 or DMSO was quantified by FACS analysis (Right). **C.** ELISA measuring the production of IL-5 and IL-13 by human ILC2 cells treated with either CRX527 or DMSO. **D.** Light microscopic images showed that the LPS-stimulated growth of ILC2 cells were inhibited by the increased dose of a specific TLR4 antagonist, LPS-RS. Each image represented one well in which 1,000 cells were initially seeded. Scale bar, 100 μm (Left). The number of human ILC2 cells treated with LPS-RS was quantified by FACS analysis (Right). **E.** ELISA measuring the production of IL-5 and IL-13 by human ILC2 cells treated with the increased doses of LPS-RS. (* P value <0.05 was considered statistically significant, unpaired t-test, ** $p < 0.01$, *** $p < 0.001$, **** $p < 0.0001$).

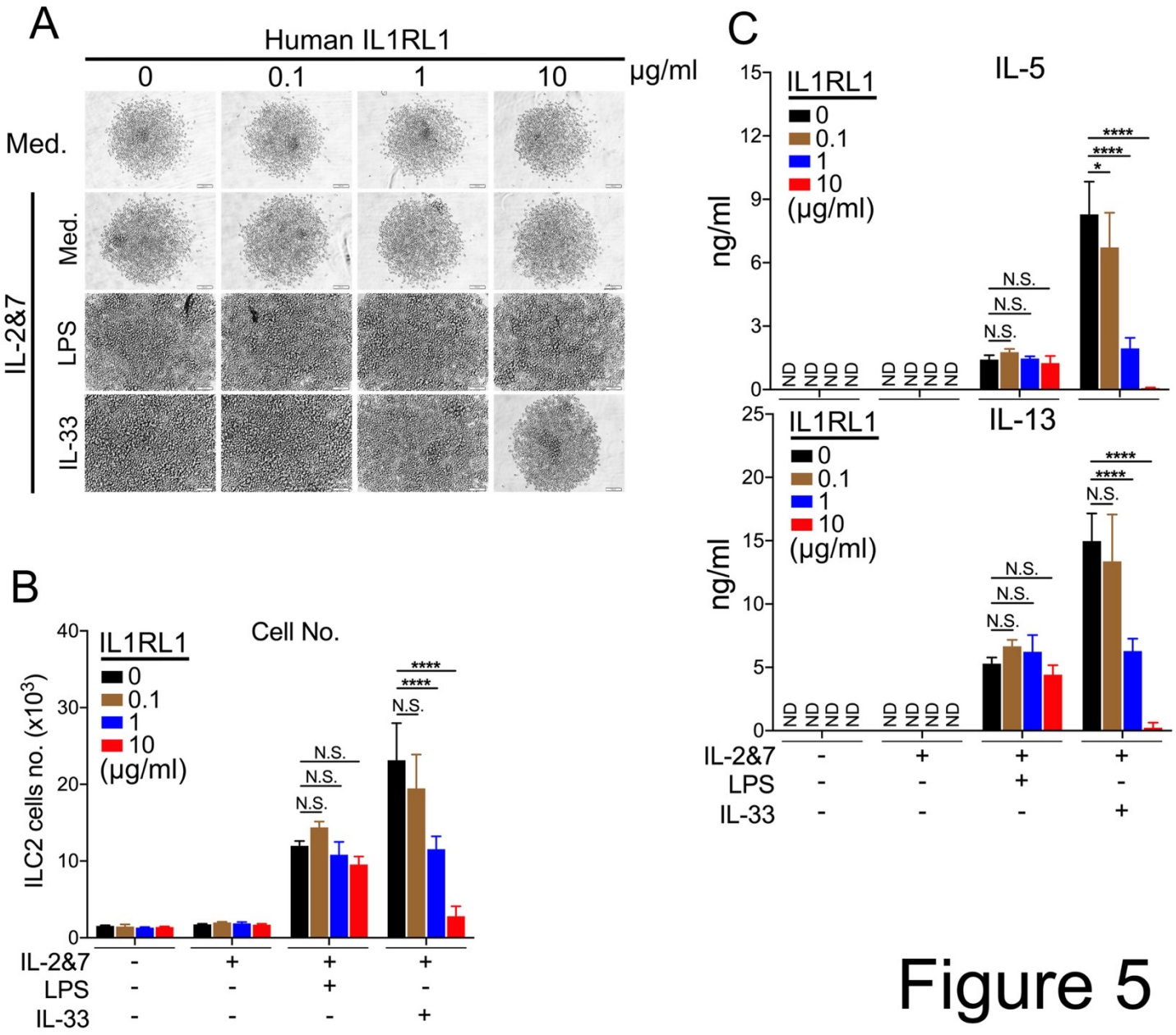

Figure 5

Figure 5. LPS-activated human ILC2 cells are insensitive to the blocking effects of recombinant protein IL1RL1, the IL-33 receptor. A. Light microscopic images showing the growth of ILC2 cells treated with the increased dose of recombinant protein IL1RL1. FACS sorted human ILC2 cells were activated with either LPS or IL-33 as indicated. Each image represented one well in which 1,000 cells were initially seeded. Scale bar, 100μm. **B.** FACS showing the number of human ILC2 cells treated with the increased dose of recombinant protein IL1RL1. **C.** ELISA measuring the production of IL-5 and IL-13 by human ILC2 cells treated with the increased dose of recombinant protein IL1RL1. (P value <0.05 was considered statistically significant, two-way ANOVA, **** $p < 0.0001$).

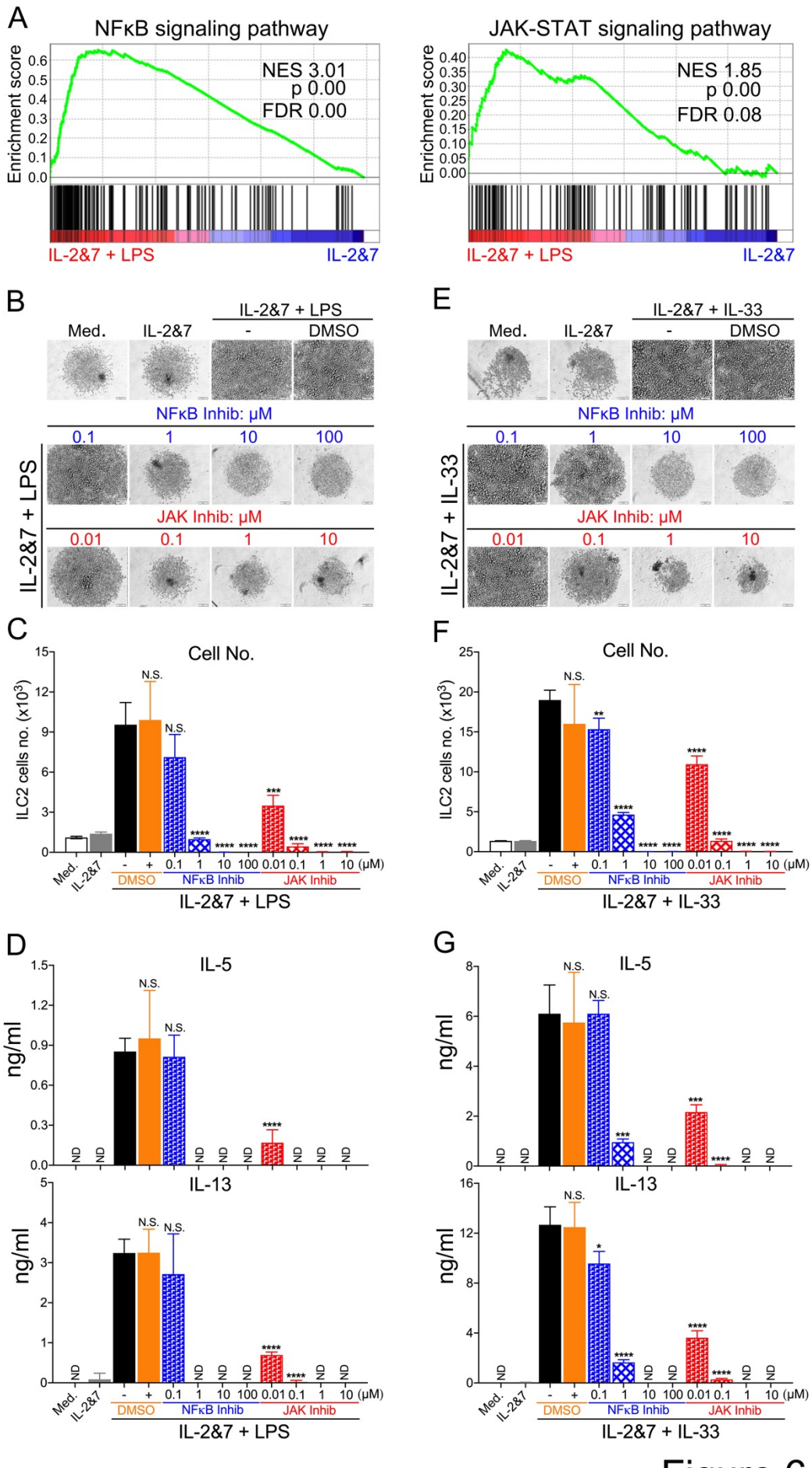
A
NFκB signaling pathway
Enrichment score
NES 3.01
p 0.00
FDR 0.00
IL-2&7 + LPS
IL-2&7
JAK-STAT signaling pathway
NES 1.85
p 0.00
FDR 0.08
B
Med.
IL-2&7
IL-2&7 + LPS
DMSO
NFκB Inhib: μM
JAK Inhib: μM
E
IL-2&7 + IL-33
C
Cell No.
ILC2 cells no. (x10³)
N.S.
DMSO
NFκB Inhib
JAK Inhib
F
D
IL-5
IL-13
ng/ml
ND
G

Figure 6

Figure 6. NF-κB and JAK pathways contribute to the proliferation and cytokine production of LPS- and IL-33-stimulated human ILC2 cells. A. Venn diagram showing the DEGs in the NF-κB and JAK-STAT pathways in human ILC2 cells stimulated with IL-2&7 plus LPS, as compared to those treated with IL-2&7 **B.** Light microscopic images showing the growth of LPS-activated ILC2 cells in the presence of the increased concentration of NF-κB- and JAK- inhibitors, or DMSO. Each image represented one well in which 1,000 cells were initially seeded. Scale bar, 100μm. **C.** FACS showing the number of LPS-activated ILC2 cells in the presence of the increased concentration of NF-κB- and JAK- inhibitors, or DMSO. **D.** ELISA measuring the production of IL-5 and IL-13 by human ILC2 cells treated with LPS in the presence of the increased concentration of NF-κB- and JAK- inhibitors, or DMSO. **E.** Light microscopic images showing the growth of IL-33-activated ILC2 cells in the presence of the increased concentration of NF-κB- and JAK- inhibitors, or DMSO. Each image represented one well in which 1,000 cells were initially seeded. Scale bar, 100μm. **F.** FACS showing the number of IL-33-activated ILC2 cells in the presence of the increased concentration of NF-κB- and JAK- inhibitors, or DMSO. **G.** ELISA measuring the production of IL-5 and IL-13 by human ILC2 cells treated with IL-33 in the presence of the increased concentration of NF-κB- and JAK- inhibitors, or DMSO. (P value≥0.05 was considered statistically insignificant, N.S., unpaired t-test, * $p < 0.05$, ** $p < 0.01$, *** $p < 0.001$, **** $p < 0.0001$).

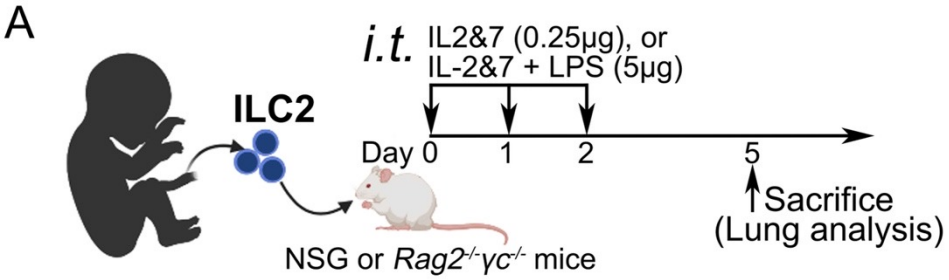
A
ILC2
i.t. IL2&7 (0.25µg), or
IL-2&7 + LPS (5µg)
Day 0
1
2
5
Sacrifice
(Lung analysis)
NSG or Rag2-/-γc-/- mice

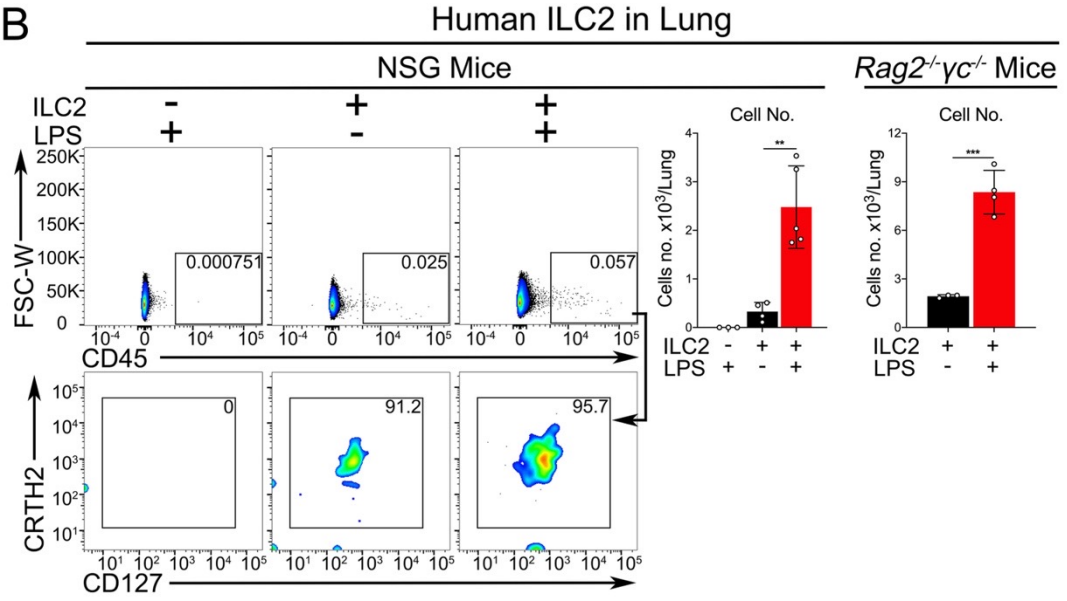
B
Human ILC2 in Lung
NSG Mice
Rag2-/-γc-/- Mice
ILC2
LPS
FSC-W
CD45
CRTH2
CD127
0.000751
0.025
0.057
0
91.2
95.7
Cell No.
Cells no. x10³/Lung

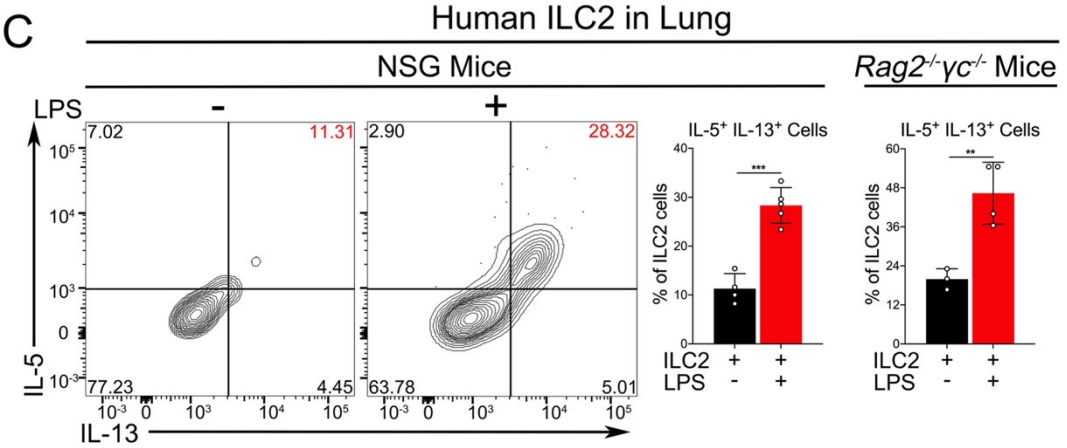
C
Human ILC2 in Lung
NSG Mice
Rag2-/-γc-/- Mice
LPS
IL-5
IL-13
7.02
11.31
77.23
4.45
2.90
28.32
63.78
5.01
IL-5+ IL-13+ Cells
% of ILC2 cells

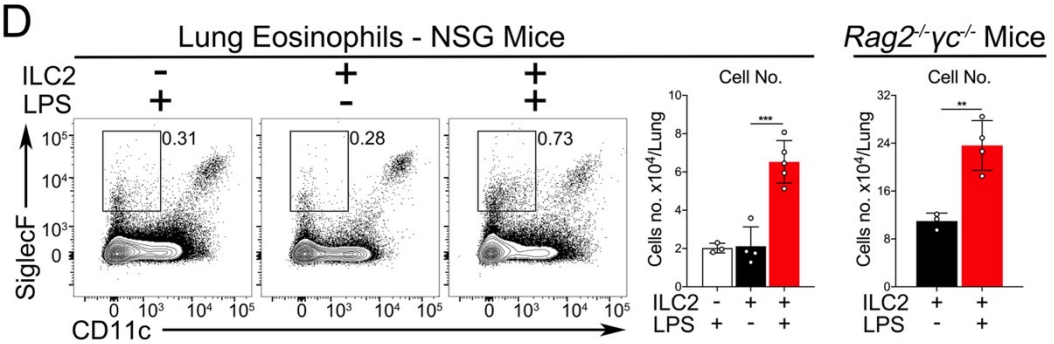
D
Lung Eosinophils - NSG Mice
Rag2-/-γc-/- Mice
ILC2
LPS
SiglecF
CD11c
0.31
0.28
0.73
Cell No.
Cells no. x10⁴/Lung

Figure 7

Figure 7. LPS could induce human ILC2 cells-mediated eosinophilic lung inflammation in humanized mouse models. A. An experimental protocol for studying the activation of human ILC2 cells by LPS in two humanized mouse models. **B.** FACS showing the number of mouse lung eosinophils in NSG or $Rag2^{-/-}\gamma c^{-/-}$ mice, which were reconstituted with human ILC2 and treated with or without LPS. **C.** Same as **B**, the percentage of IL5+IL13+-double positive human ILC2 cells in NSG or $Rag2^{-/-}\gamma c^{-/-}$ mice were analyzed by the intracellular staining. **D.** Same as **B**, FACS showing the number of lung eosinophils in NSG or $Rag2^{-/-}\gamma c^{-/-}$ mice. (unpaired t-test, ** $p < 0.01$, *** $p < 0.001$).

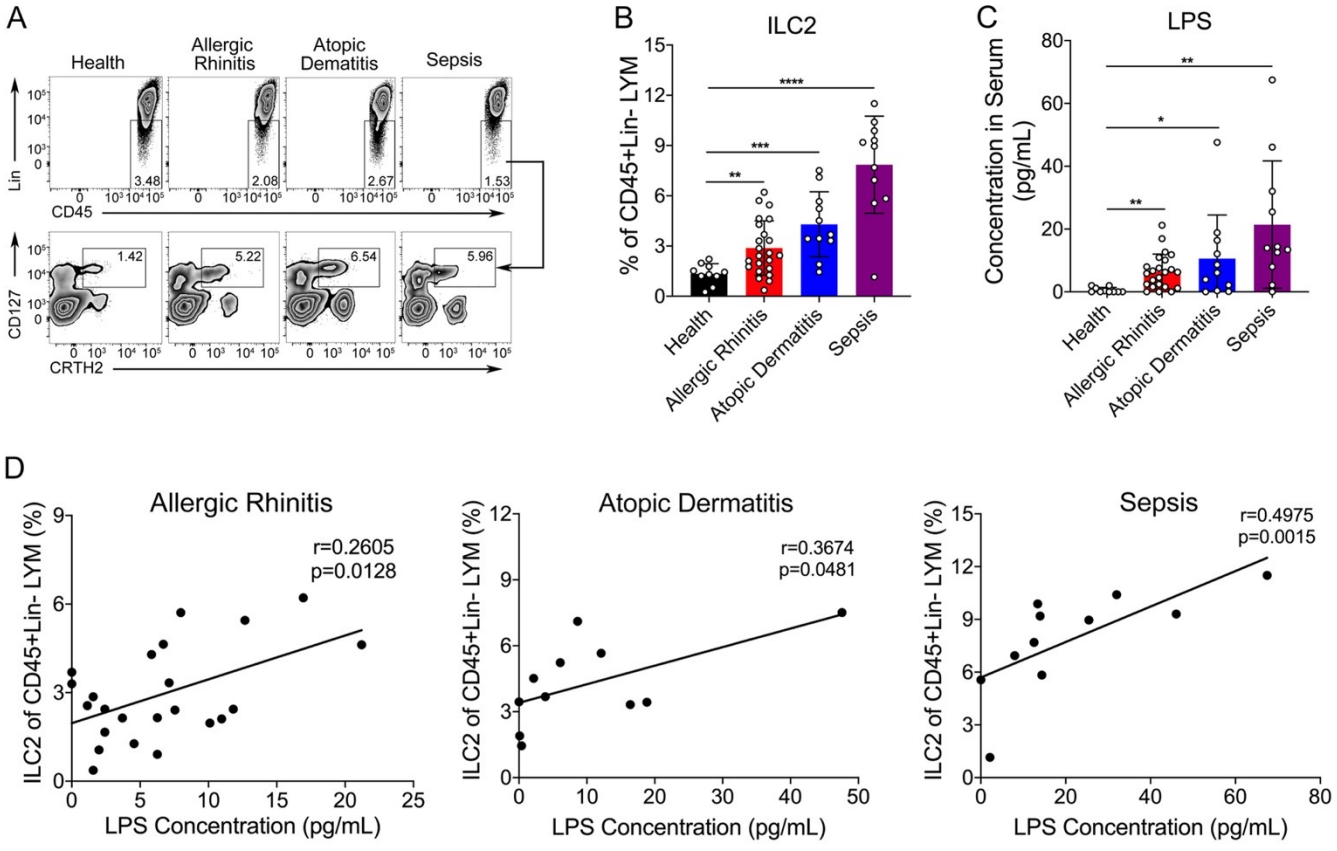

Figure 8

Figure 8. The increased percentage of ILC2 cells (% of CD45$^+$Lin$^-$ lymphocytes) associated with elevated levels of LPS in the peripheral blood of A.R., A.D. and sepsis patients. A. Human ILC2 gating strategy. Human ILC2s in peripheral blood of healthy, A.R., A.D., sepsis patients were stained with antibodies against CD45 and lineage markers (CD45$^+$Lin$^-$CRTH2$^+$CD127$^+$). **B.** The percentage of blood ILC2 cells in healthy, A.R., A.D., and sepsis patients were analyzed by FACS. **C**. The level of blood LPS in healthy, A.R., A.D., and sepsis patients were measured by ELISA. (unpaired t-test, * $p < 0.05$, ** $p < 0.01$, *** $p < 0.001$, **** $p < 0.0001$). **D**. The correlation analysis between the ILC2 number and LPS level in the peripheral blood of patients.

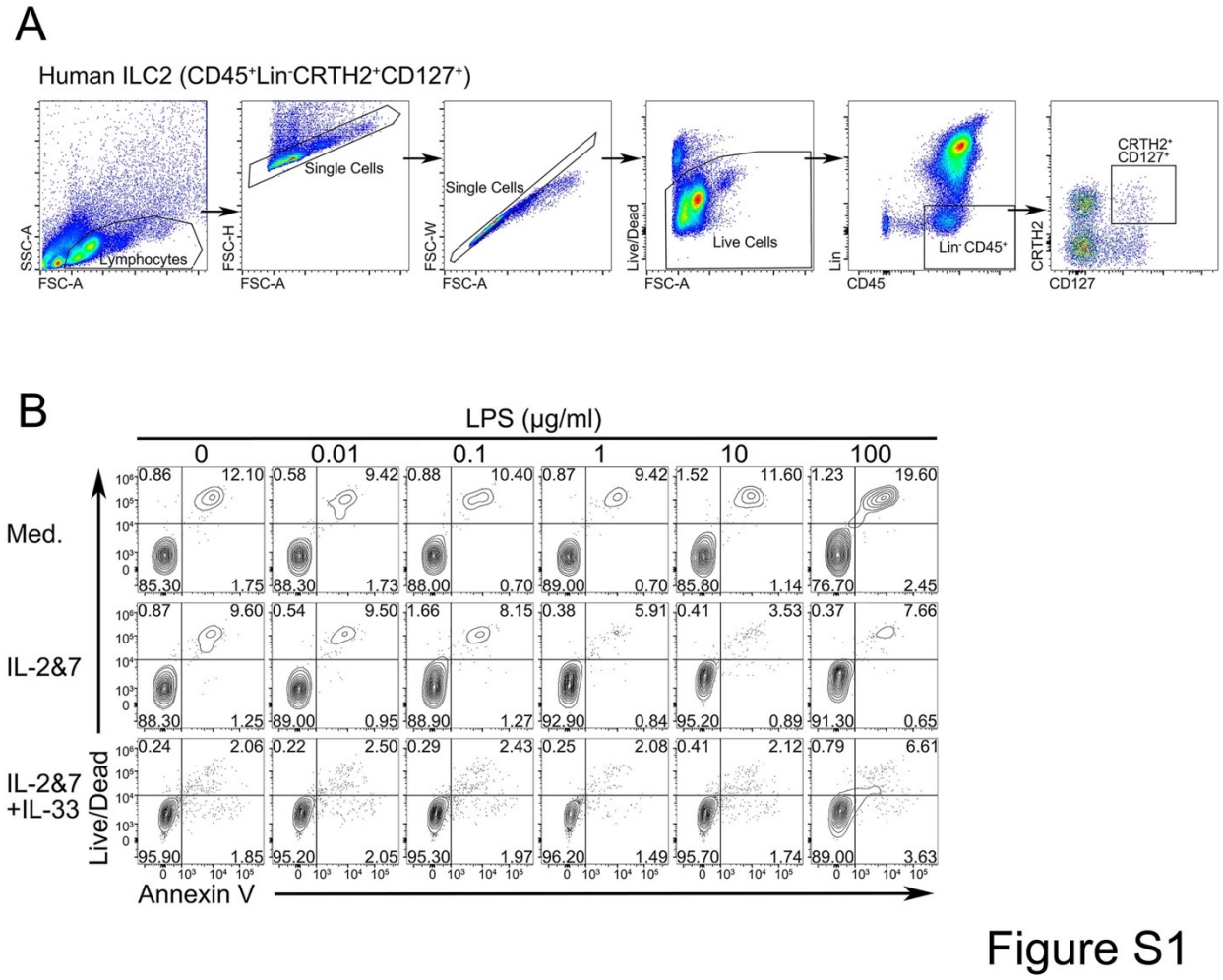

Figure S1

Fig. S1. Flow cytometry gating strategy of human ILC2 and cell death analysis of LPS-stimulated human ILC2 cells. A. Human ILC2s were isolated from peripheral blood of healthy donors PBMCs or umbilical cord blood samples CBMCs, stained with antibodies against CD45 and lineage markers ($CD45^+Lin^-CRTH2^+CD127^+$) and were sorted by the BD FACSAria. **B.** Cell death analysis of human ILC2 cells on day 3. Human ILC2 cells were treated with the increased dose of LPS as indicated. The cell death of human ILC2 cells was measured by Live/Dead dye and Annexin V staining using FACS.

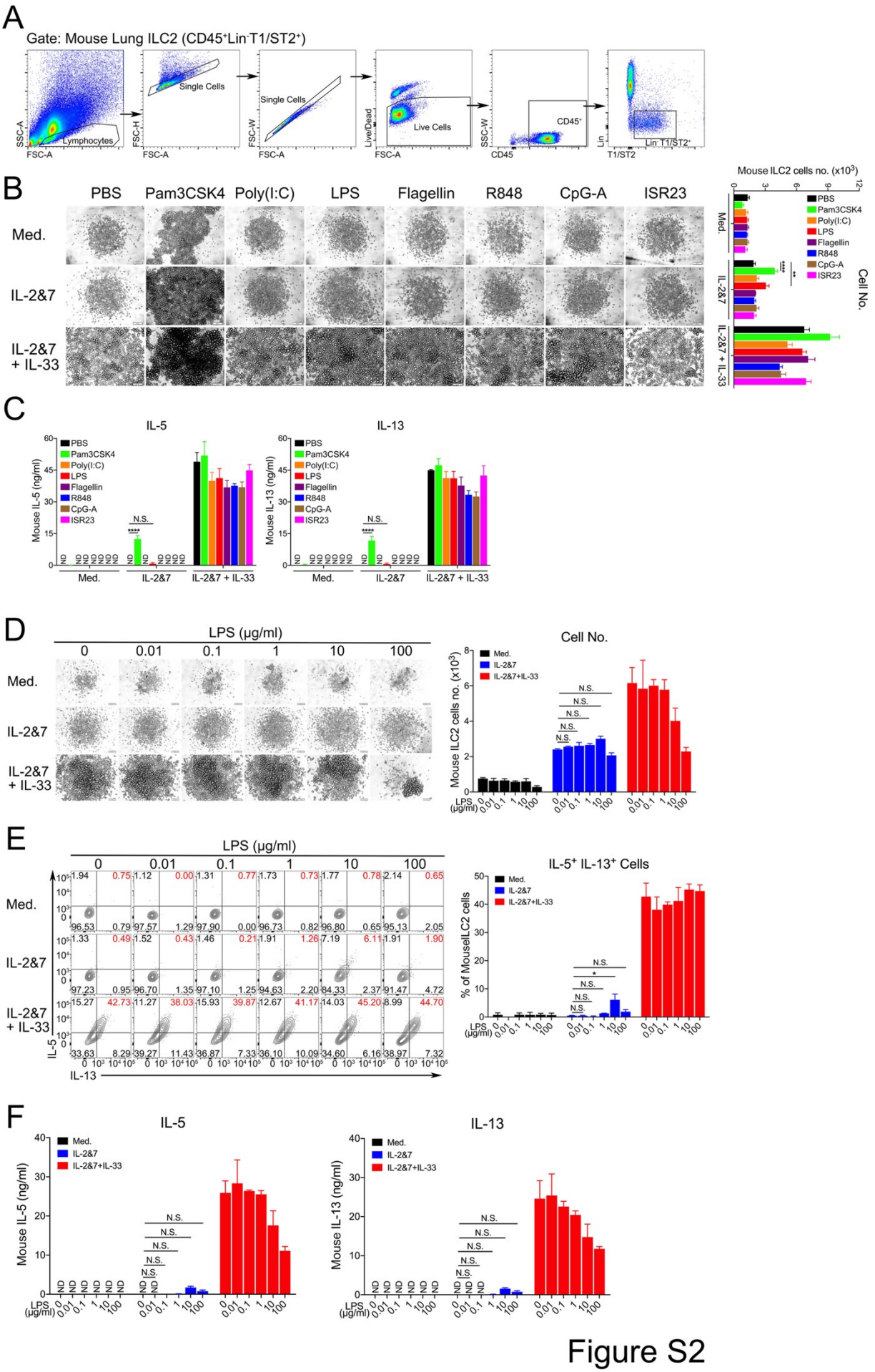
A
Gate: Mouse Lung ILC2 (CD45+Lin-T1/ST2+)
SSC-A
FSC-A
Lymphocytes
FSC-H
Single Cells
FSC-W
Single Cells
Live/Dead
Live Cells
SSC-W
CD45+
CD45
Lin-
T1/ST2+
B
PBS
Pam3CSK4
Poly(I:C)
LPS
Flagellin
R848
CpG-A
ISR23
Med.
IL-2&7
IL-2&7 + IL-33
Mouse ILC2 cells no. (x10³)
Cell No.
C
IL-5
IL-13
Mouse IL-5 (ng/ml)
Mouse IL-13 (ng/ml)
N.S.
ND
D
LPS (μg/ml)
0
0.01
0.1
1
10
100
Cell No.
Mouse ILC2 cells no. (x10³)
E
LPS (μg/ml)
IL-5
IL-13
IL-5+ IL-13+ Cells
% of MouseILC2 cells
F
IL-5
IL-13
Mouse IL-5 (ng/ml)
Mouse IL-13 (ng/ml)

Figure S2

Figure S2. LPS weakly stimulated the growth and cytokine production of mouse lung-derived ILC2. A. Mouse ILC2 gating strategy. Mouse ILC2s were isolated from mouse lungs treated with recombinant IL-33 protein (250ng/mouse, i.t.) and stained with antibodies against CD45 and lineage markers as described in the Materials and Methods. Murine ILC2s were sorted by the BD FACSAria cell sorter as CD45+Lin-T1/ST2+ cells. The purity of sorted ILC2s was determined to be greater than 95%. **B.** Light microscopic images showing the growth of ILC2 cells. Mouse ILC2 cells were treated with various TLR ligands as indicated in a 96-well round-bottom plate for 5 days. Each image represented one well in which 1,000 cells were initially seeded. Scale bar, 100 μm (Left). The number of mouse ILC2 cells treated with various TLR ligands as indicated was quantified by FACS analysis (Right). **C**. ELISA measuring the production of IL-5 and IL-13 by mouse ILC2 cells treated with various TLR ligands as indicated. **D.** LPS stimulated mouse ILC2 cells in a dose-dependent manner. Light microscopic images showing the growth of ILC2 cells treated with the increased dose of LPS as indicated (Left). The number of mouse ILC2 cells from each dose of LPS treatment was quantified by FACS analysis (Right). **E**. The representative FACS result showing the intracellular staining of IL5+IL13+-double positive mouse ILC2 cells activated by the increased dose of LPS (Left). The percentage of human ILC2 cells from each dose of LPS treatment was quantified by FACS analysis (Right). **F.** ELISA measuring the production of IL-5 and IL-13 by mouse ILC2 cells treated with the increased dose of LPS. (P value≥0.05 was considered statistically insignificant, N.S., two-way ANOVA, * $p < 0.05$, ** $p < 0.01$, **** $p < 0.0001$).

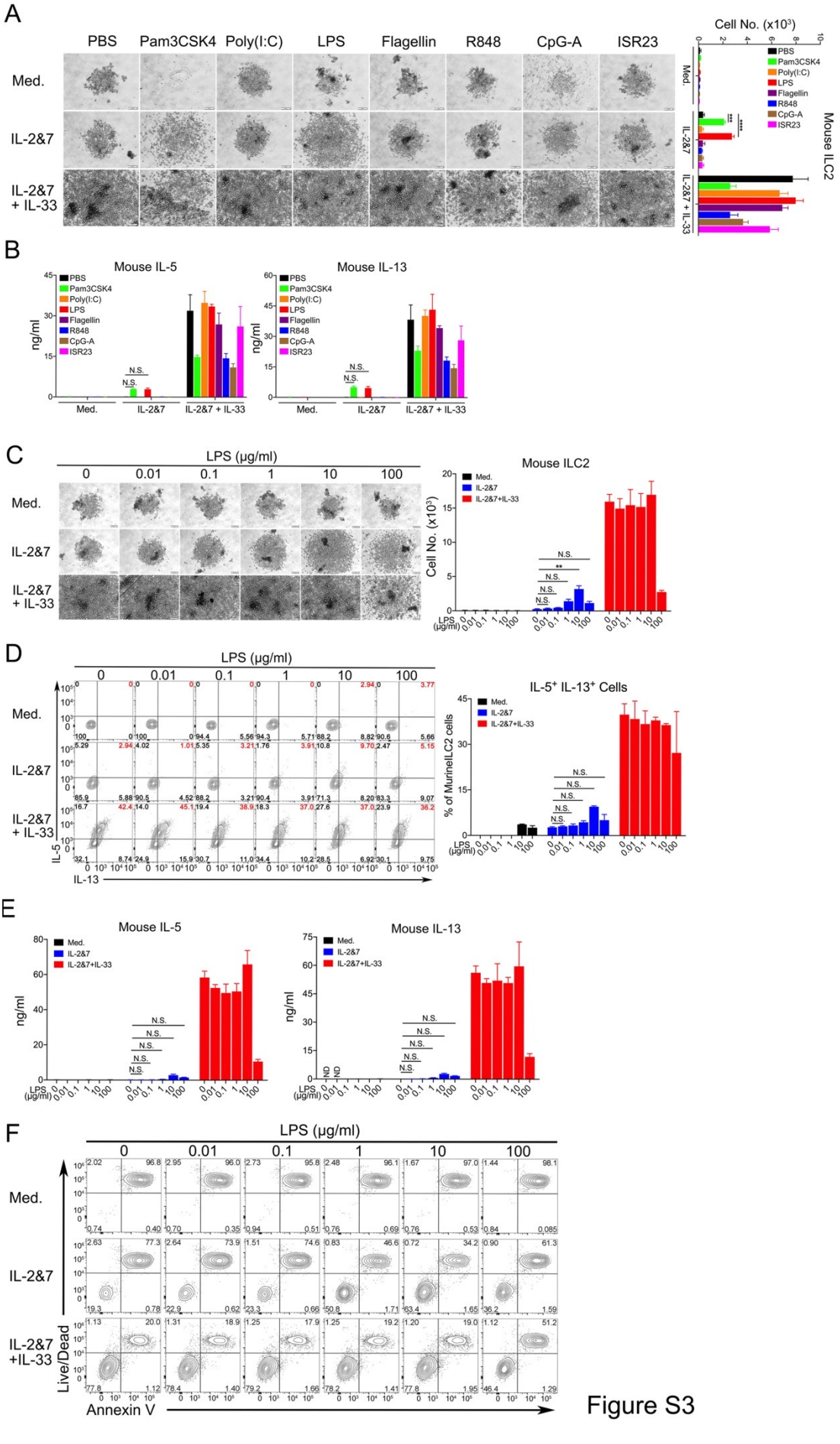
A
PBS
Pam3CSK4
Poly(I:C)
LPS
Flagellin
R848
CpG-A
ISR23
Med.
IL-2&7
IL-2&7 + IL-33
Cell No. (x10³)
Mouse ILC2
B
Mouse IL-5
Mouse IL-13
ng/ml
N.S.
C
LPS (μg/ml)
0
0.01
0.1
1
10
100
Mouse ILC2
Cell No. (x10³)
D
IL-5⁺ IL-13⁺ Cells
% of MurinelLC2 cells
IL-5
IL-13
E
Mouse IL-5
Mouse IL-13
ND
F
Live/Dead
Annexin V

Figure S3

Figure S3. LPS weakly stimulated the growth and cytokine production of mouse bone marrow-derived ILC2. A. Light microscopic images showing the growth of ILC2 cells. Mouse bone marrow-derived ILC2 cells were treated with various TLR ligands as indicated in a 96-well round-bottom plate for 5 days. Each image represented one well in which 1,000 cells were initially seeded. Scale bar, 100 μm (Left). The number of mouse ILC2 cells treated with various TLR ligands as indicated was quantified by FACS analysis (Right). **B**. ELISA measuring the production of IL-5 and IL-13 by mouse ILC2 cells treated with various TLR ligands as indicated. **C.** LPS stimulated mouse ILC2 cells in a dose-dependent manner. Light microscopic images showing the growth of ILC2 cells treated with the increased dose of LPS as indicated (Left). The number of mouse ILC2 cells from each dose of LPS treatment was quantified by FACS analysis (Right). **D**. The representative FACS result showing the intracellular staining of IL5+IL13+-double positive mouse ILC2 cells activated by the increased dose of LPS (Left). The percentage of human ILC2 cells from each dose of LPS treatment was quantified by FACS analysis (Right). **E.** ELISA measuring the production of IL-5 and IL-13 by mouse ILC2 cells treated with the increased dose of LPS. **F.** Cell death analysis of mouse bone marrow-derived ILC2 cells on day 3. Mouse ILC2 cells were treated with the increased dose of LPS as indicated. The cell death was measured by Live/Dead dye and Annexin V staining using FACS.(P value≥0.05 was considered statistically insignificant, N.S., two-way ANOVA, ** $p < 0.01$, **** $p < 0.0001$).

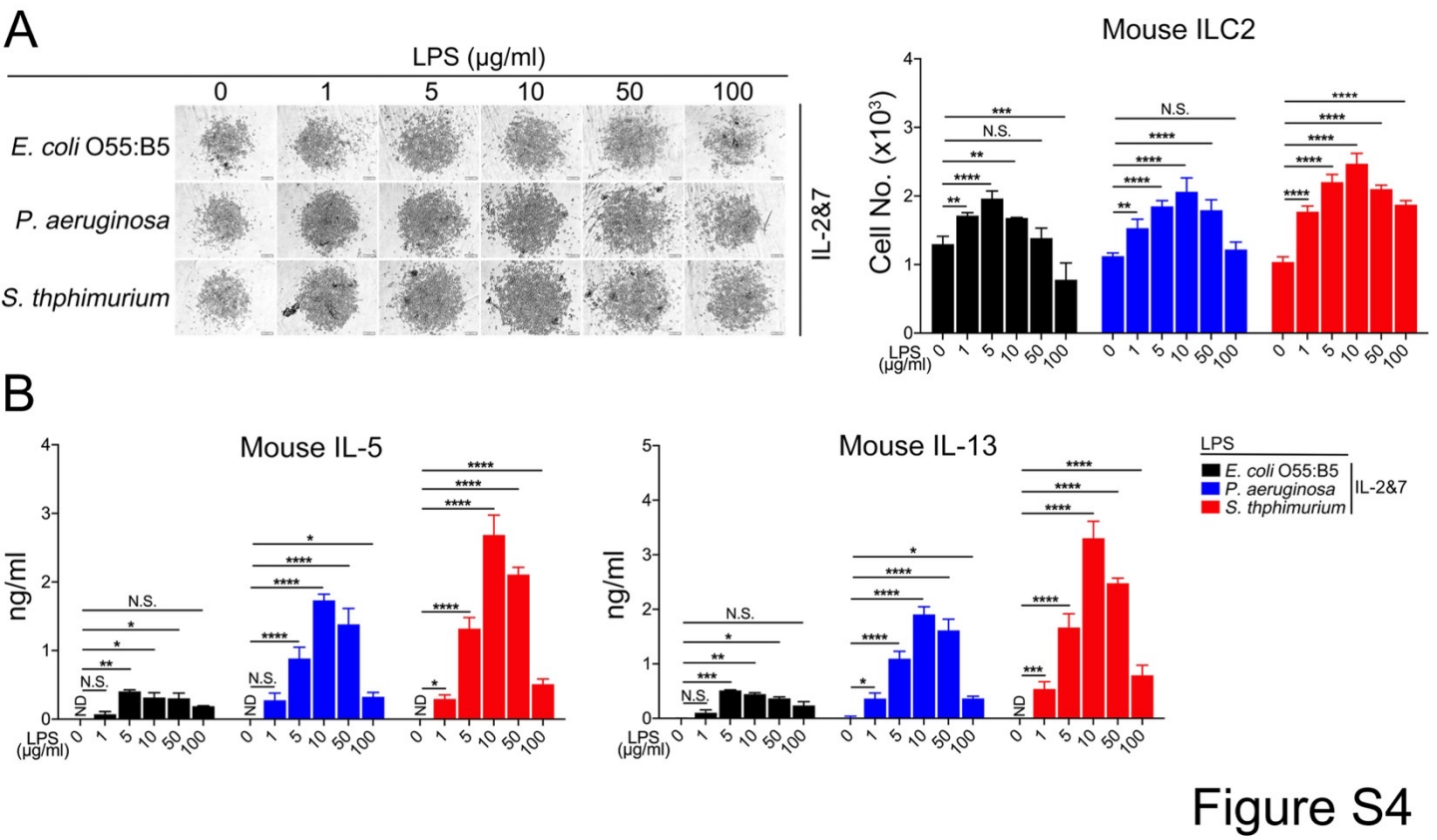

Figure S4

Figure S4. LPS from various Gram (-) bacterial species could stimulate the growth and cytokine production of mouse bone marrow-derived ILC2. A. Light microscopic images showing the growth of ILC2 cells treated with LPS isolated from *E. coli 055:B5*, *P. aeruginosa* and *S. typhimurium*. FACS sorted mouse ILC2 cells were treated with various LPS as indicated in a 96-well round-bottom plate for 5 days. Each image represented one well in which 1,000 cells were initially seeded. Scale bar, 100 μm (Right). The number of mouse ILC2 cells treated with various LPS as indicated was quantified by FACS analysis (Right). **B**. ELISA measuring the production of IL-5 and IL-13 by mouse ILC2 cells treated with various LPS as indicated. (P value≥0.05 was considered statistically insignificant, N.S., two-way ANOVA, * $p < 0.05$, ** $p < 0.01$, **** $p < 0.0001$).

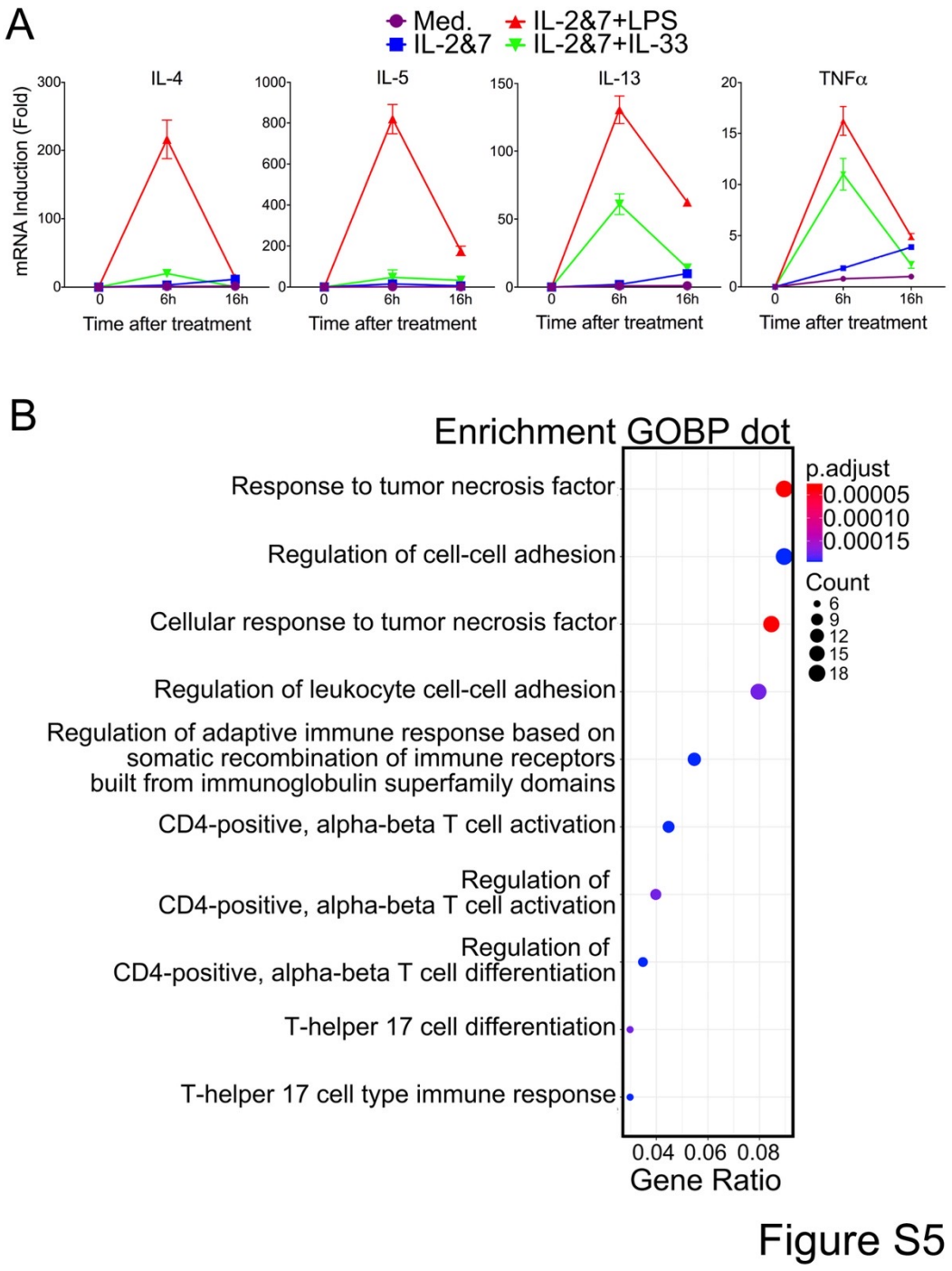

Figure S5. Gene expressions analysis of LPS-stimulated human ILC2. A. Human ILC2 cells were collected at 0, 6 and 16 hours post LPS treatment. The mRNA expression of type 2 cytokines (IL-4, IL-5 and IL-13) and TNFα were measured with RT-qPCR. **B.** Dotplot showing the enrichment analysis of Gene Ontology biological process (GOBP).

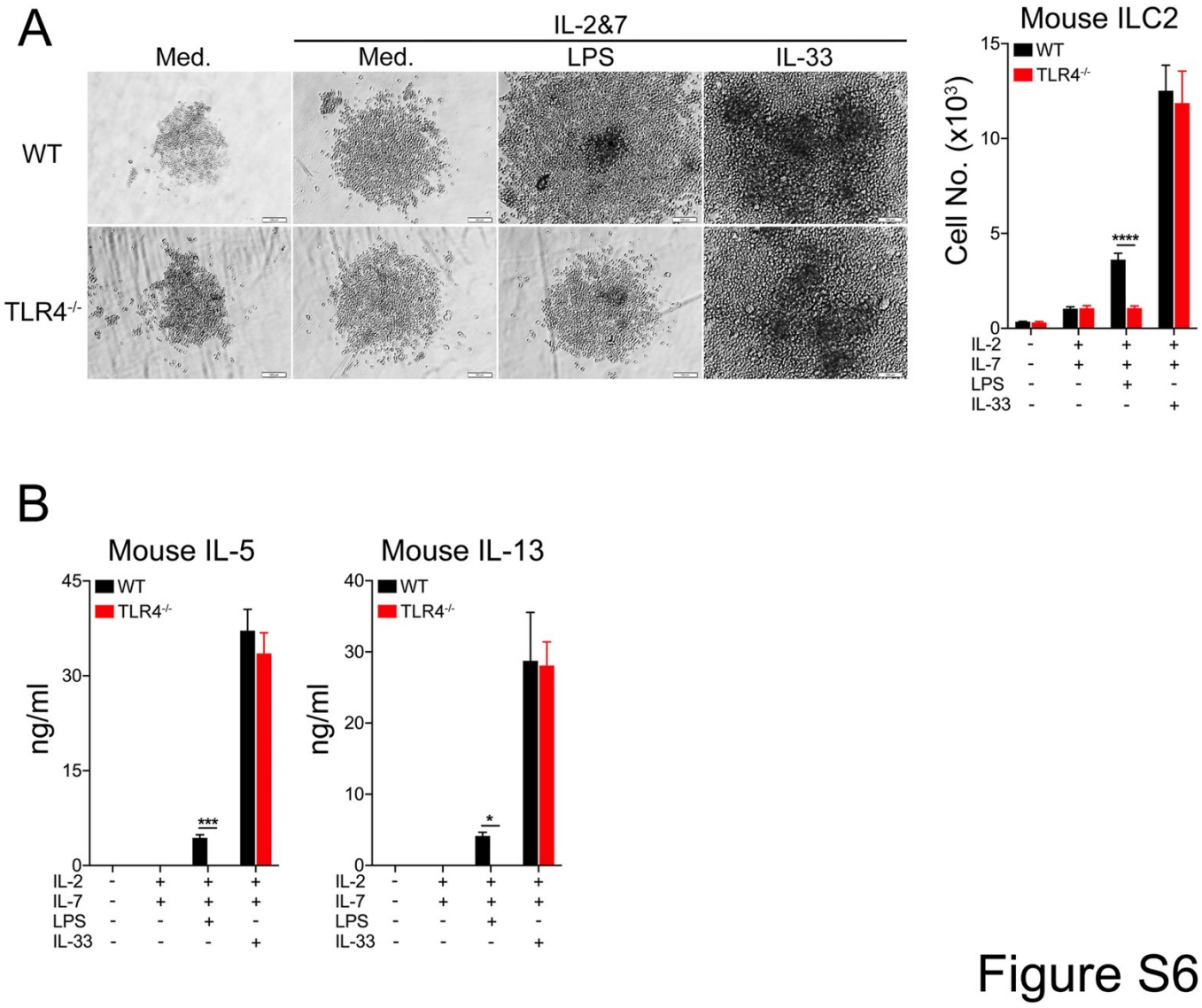

Figure S6

Figure S6. TLR4$^{-/-}$ bone marrow-derived ILC2 was unresponsive to LPS stimulation. A. Light microscopic images showing the growth of ILC2 cells. FACS sorted WT and TLR4$^{-/-}$ ILC2 cells were treated with LPS in a 96-well round-bottom plate for 5 days. Each image represented one well in which 1,000 cells were initially seeded. Scale bar, 100 μm (Left). The number of bone marrow-derived ILC2 cells after LPS treatment was quantified by FACS analysis (Right). **B**. ELISA measuring the production of IL-5 and IL-13 by ILC2 cells after LPS stimulation. (unpaired t-test, * $p < 0.05$, *** $p < 0.001$, **** $p < 0.0001$).

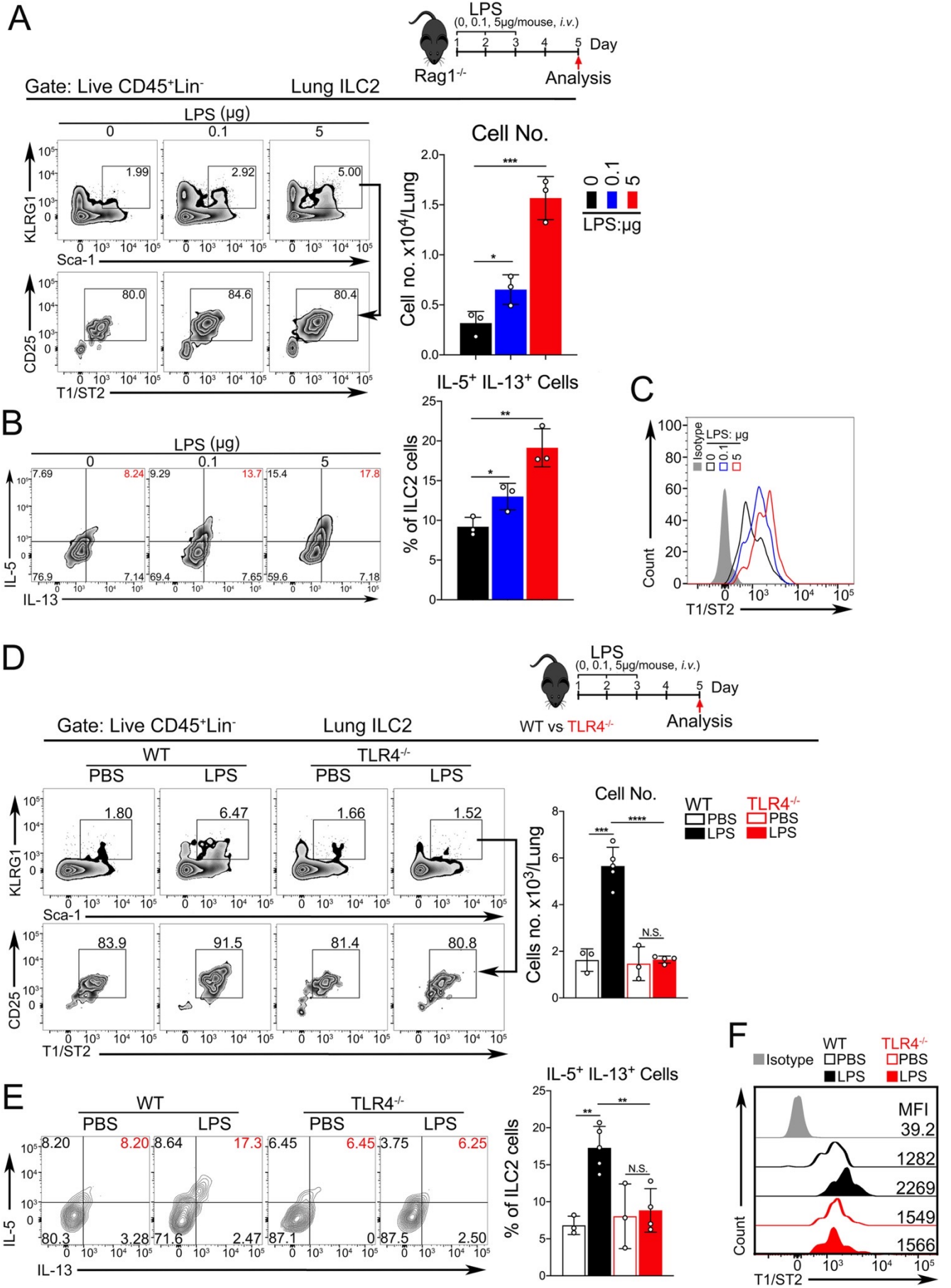
A
LPS
(0, 0.1, 5μg/mouse, i.v.)
1 2 3 4 5 Day
Rag1-/-
Analysis
Gate: Live CD45+Lin-
Lung ILC2
LPS (μg)
0
0.1
5
KLRG1
Sca-1
1.99
2.92
5.00
CD25
T1/ST2
80.0
84.6
80.4
Cell No.
Cell no. x10^4/Lung
LPS:μg
B
IL-5+ IL-13+ Cells
% of ILC2 cells
IL-5
IL-13
7.69
8.24
9.29
13.7
15.4
17.8
76.9
7.14
69.4
7.65
59.6
7.18
C
Isotype
LPS: μg
Count
T1/ST2
D
LPS
(0, 0.1, 5μg/mouse, i.v.)
1 2 3 4 5 Day
WT vs TLR4-/-
Analysis
Gate: Live CD45+Lin-
Lung ILC2
WT
TLR4-/-
PBS
LPS
1.80
6.47
1.66
1.52
83.9
91.5
81.4
80.8
Cell No.
Cells no. x10^3/Lung
N.S.
E
8.20
8.20
8.64
17.3
6.45
6.45
3.75
6.25
80.3
3.28
71.6
2.47
87.1
0
87.5
2.50
IL-5+ IL-13+ Cells
% of ILC2 cells
F
Isotype
MFI
39.2
1282
2269
1549
1566
Count
T1/ST2

Figure S7

Figure S7. Systemic delivery of LPS into Rag1$^{-/-}$ and WT, but TLR4$^{-/-}$ mice triggered the growth, effector function and enhanced ST2 expression of ILC2 . A. FACS showing the number of mouse lung ILC2 in Rag1$^{-/-}$ mice, which were intravenously treated with increased dose of LPS as indicated. The gating strategy was shown on the right. **B.** The percentage of IL5+IL13+-double positive human ILC2 cells in Rag1$^{-/-}$ mice were analyzed by the intracellular staining. **C.** FACS showing the ST2 expression level on Rag1$^{-/-}$ ILC2 after LPS stimulation. **D.** Same as **A**, FACS showing the number of mouse lung ILC2 in WT and TLR4$^{-/-}$ mice, which were intravenously treated with LPS. The gating strategy was shown on the right. **E.** The percentage of IL5+IL13+-double positive human ILC2 cells in WT and TLR4$^{-/-}$ mice were analyzed by the intracellular staining. **F.** FACS showing the ST2 expression level on ILC2 of WT and TLR4$^{-/-}$ mice after LPS stimulation. (P value≥0.05 was considered statistically insignificant, N.S., unpaired t-test, * $p < 0.05$, ** $p < 0.01$, *** $p < 0.001$, **** $p < 0.0001$).

Table S1. Patient information of allergic rhinitis

			symptom					Specific IgE		
No.	gender	age	nasal obstruction	rhinocnesmus	sneeze	rhinorrhea	concomitant symptoms	Dermatophagoides farinae (KUA/L)	Dermatophagoides pteronyssinu (KUA/L)	mean fractional exhaled nitric oxide (ppb)
1	F	23	N	Y	Y	Y	eye itching	24.4	22.8	NA
2	M	9	Y	Y	Y	Y	None	35.1	48.3	NA
3	M	23	Y	Y	Y	Y	None	26.1	22.9	137
4	M	30	Y	Y	Y	Y	None	0.46	0.52	453
5	M	28	Y	Y	Y	Y	None	0.39	0.45	510
6	M	13	Y	Y	Y	Y	eye itching	44.3	44.9	NA
7	F	16	Y	Y	Y	Y	None	5.76	4.03	257
8	F	23	Y	Y	Y	Y	None	10.4	15.5	412
9	M	13	Y	Y	Y	Y	None	63.8	49.6	466
10	M	16	Y	Y	Y	Y	None	0.57	0.61	460
11	F	20	Y	Y	Y	Y	eye itching	0.01	0.02	397
12	M	33	N	Y	Y	Y	None	0.17	0.2	465
13	F	59	Y	N	Y	Y	None	0	0.03	NA
14	M	12	Y	N	Y	Y	None	35.5	20	NA
15	F	40	N	Y	Y	Y	None	15.6	21.3	NA
16	M	27	Y	Y	Y	Y	None	0.02	0.04	NA
17	F	17	Y	Y	Y	Y	None	0.67	0.61	NA
18	F	16	Y	Y	Y	Y	eye itching	92.7	>100	234
19	M	42	Y	Y	Y	Y	eye itching	0.5	0.37	445
20	M	19	Y	Y	Y	Y	eye itching	7.51	7.2	398
21	M	15	Y	Y	Y	Y	Epistaxis	0.34	0.38	364
22	M	12	Y	Y	Y	Y	eye itching	45.6	45.8	579
23	M	12	Y	Y	Y	Y	eye itching	26.3	29.2	790

Table S2. Patient information of atopic dermatitis

No.	gender	age	symptom	total IgE	serum IgE (IU/mL)
1	F	28	Erythema, wheal, pruritus	+	NA
2	F	56	Erythema, wheal, pruritus	NA	100.1
3	M	12	Erythema, wheal	+	534.9
4	F	25	wheal, pruritus	+	8.5
5	F	14	wheal, pruritus	+	161.2
6	F	42	wheal, pruritus	+	26.9
7	M	29	rash，wheal	NA	NA
8	F	20	rash，wheal	NA	NA
9	F	50	rash，wheal	NA	NA
10	F	26	rash，wheal	NA	NA
11	M	52	rash，wheal	NA	NA

Table S3. Patient information of sepsis

No.	gender	age	History of tobacco use	past history	source of sepsis	neutrophil-to-lymphocyte ratio	white blood cell count (*10^9/L)	Percentage of neutrophils	Percentage of lymphocytes	serum creatinine concentration (μmmolNAL)	APACHEII score	culture result
1	M	55	N	None	urinary tract	20.2	20.5	83.2%	9.3%	65.8	NA	positive
2	M	64	N	Hepatitis E virus infection	other	21.3	9.4	90.4%	4.3%	232	NA	negative
3	F	57	N	coronary heart disease, diabetes, renal insufficiency	lung	8.9	10.7	83.2%	9.3%	658	NA	positive
4	M	60	Y	dyslipidemia	abdomen	18.3	5.9	93.2%	5.1%	197.3	20	positive
5	F	55	N	None	abdomen	8.7	16.3	85.3%	9.8%	72.2	7	positive
6	M	63	N	renal insufficiency	lung	11.9	9.1	91.2%	7.7%	181.8	28	positive
7	F	64	N	hypertension	lung	17.3	25.0	90.0%	5.2%	57	19	positive
8	M	64	N	hypertension	abdomen	15.5	7.4	87.8%	5.4%	53.5	10	positive
9	M	43	N	diabetes	other	7.5	12.2	79.5%	10.7%	86	NA	negative
10	M	58	Y	hypertension、dyslipidemia	abdomen	5.8	13.3	78.2%	13.5%	102.9	5	negative
11	F	62	N	hypertension、diabetes	urinary tract	27.0	11.6	93.1%	3.4%	665.5	11	positive